OPTIMAL MITIGATION OF GEOMAGNETICALLY INDUCED CURRENT EFFECTS IN POWER SYSTEMS CONSIDERING TRANSFORMER THERMAL LIMITS

ANUSHA LAMICHHANE

A THESIS SUBMITTED TO THE FACULTY OF GRADUATE STUDIES
IN PARTIAL FULFILMENT OF THE REQUIREMENTS
FOR THE DEGREE OF
MASTER OF APPLIED SCIENCE

GRADUATE PROGRAM IN ELECTRICAL ENGINEERING AND COMPUTER SCIENCE
YORK UNIVERSITY
TORONTO, ONTARIO

SEPTEMBER 2022

Abstract

An efficient energy transfer from the solar wind into the earth's space environment causes temporary disturbance to the earth's magnetosphere. Solar flares and coronal mass ejections (CME) of charged and magnetized particles can disturb the earth's magnetic field and cause geomagnetic disturbance (GMD). GMDs are of particular concern as they give rise to geomagnetically induced currents (GIC) which have adverse effects on the national power grid and potentially damage transformers on the grid.

GIC flowing along transmission lines and through the transformers in power systems can be attributed to problems ranging from overheating of power transformers, harmonic generation, and voltage collapse due to the half-cycle saturation of power transformers. To prevent the power system and its equipment from the adverse effects of GMD, blocking device (BD) can be placed to block the GIC flow in the transformers. However, BD placement is a complex problem, and the cost of BD is very high, so optimization techniques should be employed for BD placement to minimize the number and costs of BDs. Although there has been research on placing blocking devices and their optimal placement, none of them considers the hotspot temperature rise in transformers during GIC. Therefore, Voltage violation and rise in hotspot temperature of transformers are the main concerns in this thesis. This work presents two approaches for the optimal placement of blocking devices on the neutral of high voltage

transformers to prevent the power system from the impacts of GIC caused by geomagnetic disturbance. The thesis focuses on the optimization problem based on overheating of power transformers due to GIC and maintaining the hotspot temperature of transformers within the limit, as well as maintaining the voltage profile of the power system.

The problem is formulated by first calculating the GIC and increased reactive power demand of each transformer during the GIC flow, performing power flow analysis, checking if system voltage has been violated, calculating the transformers' windings and metallic hotspot temperatures, checking if the limits are reached, and optimally placing BDs on selective transformers such that the hotspot temperature of transformers is within maximum limits, and the system voltage is recovered above minimum permissible voltage. The optimization is done using the Surrogate optimization and Genetic algorithm of the MATLAB optimization toolbox and made sure that the number of BDs is minimized. A comparative analysis is done from the results obtained from both of the methods.

The findings of the thesis highlight the optimization approach for the placement of blocking devices that takes into account the hotspot temperature rise of transformer tie-plates and windings and a realistic criterion that includes the cost of the repair or replacement of transformers based on the hotspot temperature rise of transformers into the optimization approach. The thesis presents the selection criteria for the two optimization solvers, surrogate optimization and genetic algorithm, after researching and reviewing different solvers from the MATLAB optimization toolbox. The total cost of BD placement is reduced where the total load is reduced to some extent based on different levels of geoelectric field (E) to maintain the bus voltages above minimum permissible voltage, and the cost can be calculated based on the loss of load, and extra number of BDs can be avoided. The results obtained from

surrogate optimization are proved to be effective and efficient as the total number of BDs resulting from surrogate optimization is less than the total number of BDs resulting from genetic algorithm. The nature of genetic algorithm is stochastic in nature, the result not converging to the global minimum, and the time taken by genetic algorithm for the program execution were major drawbacks. In contrast, the characteristics of surrogate algorithm, such as a result, proved to be converging, non-stochastic in nature, unlike genetic algorithm, and comparatively less time consuming than genetic algorithm proving surrogate optimization to be more reliable and efficient.

Acknowledgements

I want to express my sincere gratitude to my advisor Dr. Afshin Rezaei-Zare for his expert guidance, constant support, and encouragement throughout my MASc thesis research. This work would not have been possible without his supervision. I have been extremely fortunate to work under his supervision and learned a lot from him with his knowledge, skills, and grand vision.

I am incredibly thankful to my internal member Dr. Ali Asgary for his advice, encouragement, and generous support. His feedback has always shown me the right research direction and motivated me to become a better student. In addition, I wish to thank Dr. Houshang Karimi for serving as my committee member and for his valuable time and support throughout the process.

Although no words can express my appreciation for my family, I would like to pay special and profound gratitude to my parents and my sister. Their love and encouragement have enabled me to accomplish this research. My heartiest thanks to my graduate studies friends, Subrina Shawlin and Samy Elias, for providing me with wise advice and continuous support whenever needed. Lastly, I appreciate the motivation and encouragement offered by my friends Dhiraj Basnet, Bhawesh Pokharel, and Prabin Adhikari throughout the process.

Table of Contents

List of Tables

List of Figures

Abbreviations

AEP	-	American Electric Power
BD	-	Blocking Device
CME	-	Coronal Mass Ejection
E	-	Geoelectric Field
EHV	-	Extra-High Voltage
GA	-	Genetic Algorithm
GIC	-	Geomagnetically Induced Current
GMD	-	Geomagnetic Disturbance
HV	-	High Voltage
LV	-	Low Voltage
NBD	-	Neutral Blocking Device
SO	-	Surrogate Optimization
SVC	-	Static Var Compensator

Chapter 1

Introduction

1.1 Motivation

Major disturbance in the earth's magnetosphere is caused by the release of energy from solar disturbance. Solar storms sometimes occur naturally and can interact and affect the earth's magnetic field, called geomagnetical disturbance (GMD). The geomagnetic disturbances (GMDs) create a variable electric field at the ground level, called a geoelectric field. The geoelectric field creates potential differences across the long conductors like power system transmission lines, and thus geomagnetically induced current (GIC) flows through the power system.

GIC is a potential threat to the power system as the flow of GIC through the transformers and transmission lines negatively affects power system stability and availability. The two most significant issues that need to be taken care of are the voltage instability and the rise in

hotspot temperature of transformers during the flow of GIC [1–3]. The flow of GIC through the high voltage power transformers causes half-cycle saturation of transformers. As a result, transformers turn themselves into large shunt reactive loads and absorb high reactive power. It can result in the tripping of supporting reactive devices by the protection and control system, thus leading to a significant loss of reactive power support and voltage instability [1, 3, 4]. Depending on the magnitude, frequency, and duration of GIC, overheating develops on the winding and structural parts of the transformers as a greater share of flux leaks out beyond the core due to half-cycle saturation and induces additional eddy currents in various parts of the core and windings, including metallic structural parts such as tie-plate. The life of insulation decreases with the overheating of transformers, potentially damaging expensive power transformers and even causing blackouts. Therefore, it is essential to model the flow of GIC, calculate the reactive power absorbed by transformers, calculate the temperature rise in the transformer hotspot during the flow of GIC, and determine the necessary solution to this huge problem in the power grid.

Placing blocking devices (BDs) is a long-term solution to block the GIC. But placing BDs is a complex concern as the cost of BD is very high and can make the condition even worse if not placed without enough research. Installation of blocking devices on a particular transformer can redirect the flow of GIC to the neighboring transformers as all power transformers have a path to the ground at their high-voltage side. It can worsen the power system's situation and exacerbate the voltage instability situation and high temperature rise on the transformer's hotspot. So, the placement of BDs should be well optimized without violating any constraints for the efficient operation of the power system and its equipment. There is a lot of literature on the placement of BDs [5–8], but there is only a little research on the optimal placement of BDs [9, 10]. Although a couple of papers address the optimal placement problem and

have made some effort in the sector, the articles do not address the thermal limit of the transformer hotspot. There has been scant or no analysis on the placement of BDs considering the thermal limitations of transformers. Since overheating of transformer structural parts and winding is one of the most prominent effects of GIC that can damage expensive high voltage transformers, the hotspot temperature of transformers should be considered for reliability and proper functioning of the power system in the optimization process of BD placement. This thesis proposes an optimization approach for the blocking device placement in such a way that the transformer hotspot temperature limit is not reached, and the voltage profile of the power system is maintained.

1.2 Thesis Organization

The remainder of the thesis is organized into the following chapters:

- Chapter 2 provides background on how GMD occurs and gives rise to GIC. The impacts of GIC on the power system and the GMD- related problems are well explained in the literature review. In addition, it provides background on the possible remedies that can be pursued to block the GIC, most importantly blocking devices and why and how BD should be placed on the power grid to mitigate the adverse effects of GIC.

- Chapter 3 describes the study system where the research is done, where the GIC is calculated first and later followed by other calculations such as calculating the bus voltages and hotspot temperature of transformers. The calculation of GIC is well explained in this chapter. The chapter also explains the thermal assessment of

transformers in the power system and how transformers' hotspot temperature rise is calculated using the study system, as mentioned in this chapter. The study system includes GPS coordinates of substations, transformer data, and transmission line data.

- Chapter 4 presents the approach to optimize the placement of blocking devices to block the flow of GIC through the transformers and transmission lines. The flowchart in this chapter explains the optimization process undertaken in this thesis. Two methods are used to do the optimization, surrogate optimization (SO) and genetic algorithm (GA) from MATLAB optimization toolbox.

- Chapter 5 presents the results of the simulation done in MATLAB. The voltage at different buses during the GMD event, the rise in hotspot temperature at the transformers for different levels of geoelectric field (E), $E = 1\,V/km$ to $E = 8\,V/km$ are presented in this chapter. The optimization results are presented, i.e., the optimized total number of BDs to be placed and the candidate transformers at each intensity of E. The improvement in bus voltages and hotspot temperature of transformer tie-plate and winding after the BD placement are also presented.

- Chapter 6 summarizes the work carried out in the thesis with the conclusion and future work that can be done.

Chapter 2

Literature Review

2.1 Geomagnetically Induced Current

The sun sometimes emits enormous bursts of energy in the form of solar flares and coronal mass ejection (CME). These solar disturbances can release high-energy solar flares that exchange energy from the solar wind to the earth's space environment [11]. The charged particles are produced and move in the conductive ionosphere, and current flow in the electrojets [12]. The coronal mass ejection carries its own current and magnetic field and interacts with the earth's magnetic field. As a result, the solar wind perturbs the earth's outer surface, causes major disturbance in the earth's magnetosphere, and affects the earth's magnetic field, the phenomenon called Geomagnetic Disturbance (GMD). The intensity of geomagnetic disturbance depends on the flare's magnitude, the direction in which the particles are emitted, and the orientation of the magnetic field. During geomagnetic disturbances,

variations in the electrojet (at frequencies in the order of 0.1 mHz − 0.1 Hz) and magnetic field variations induce voltages in relatively long conductors at the ground level. The wires of an HV transmission line are grounded through the neutral connection of transformers at the line terminals; as a result, a closed loop or return path is formed, and current will circulate, which is referred to as geomagnetically induced current (GIC). This quasi-dc current enters and exits the power system at the transformer's grounds, disrupts the normal operation of the power system, and even causes equipment damage in some cases. GIC not only disrupts the power system operation but also disrupts the operation of other conducting networks such as communication cables and pipelines [13]. The flow of GIC in a power network is shown in Figure 2.1.

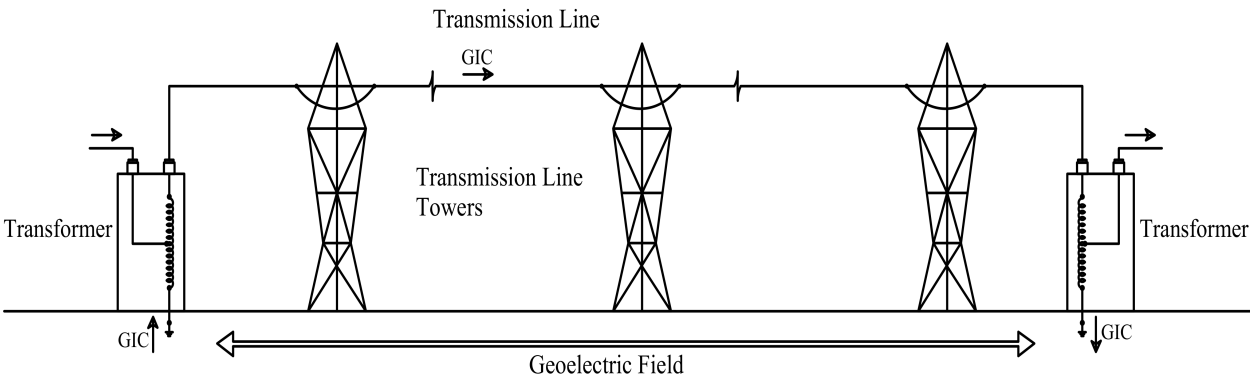

Figure 2.1: GIC flow in power network.

The first reported effects of GIC on power systems occurred during a magnetic storm in 1940 [13]. Disturbances in power systems were reported by companies in New England, New York, eastern Pennsylvania, southern and eastern parts of Minnesota, and Ontario and Quebec. Significant effects on power systems were noted during major geomagnetic storms in February 1958 and August 1972, and lesser effects were recorded during other

weaker disturbances. One of the significant disturbances occurred on March 13, 1989, that led to the collapse of the Hydro Quebec system and caused a nine-hour power disruption to six million people and was estimated to cost $6 billion (Canadian dollars) [2, 11, 13–16]. The resulting harmonics caused the tripping of several static compensators, i.e., system components essential for maintaining the dynamic stability of the network one after another. Loss of this equipment led to a severe voltage drop, and the system became totally unstable, resulting in a trip out of all the power lines coming from James Bay and the collapse of the system [2, 13, 16]. The risk to which Italian infrastructures are exposed due to GIC events is presented in [17]. The preliminary risk assessment of space weather-related GIC activity to the Australian power network is presented in [18]. [19] gives an overview of the GMD physical process and its influence on power systems. It performs an explicit numerical assessment of potential GIC values and their impacts on the grid for the Swiss Transmission Network. [20] describes a thought process and the beginnings of a methodology for global risk assessment, like independently determining the probability of the event and the consequence as represented in an estimated economic impact.

2.2 Impacts of GIC

The reason geomagnetic disturbances are particularly concerning to the power grid is geomagnetically induced current (GIC). GIC is caused by geomagnetic disturbance causing electric current variations in the magnetosphere and the ionosphere, which then cause effects on the Earth's magnetic field. This introduces currents to be induced in conductors such as power lines which will then impact and pose a threat to the power grid transformers [1, 11,

21, 22]. GIC is called quasi dc currents as they have an extremely low frequency of about $0.1\ mHz\ -\ 0.1\ Hz$. The risks associated with GIC are highly dependent on the characteristics of GMD events and parameters of the power grid [23], including geomagnetic latitude, power grid topology, ground conductivity, geoelectric field magnitude and orientations, line resistance. The transmission line length and line orientation alignments with corresponding geoelectric fields are considered key topological parameters that influence GIC magnitudes in the electric grid [24] which is presented in chapter 3 in the calculation of GIC.

The flow of GIC through the transmission lines and transformers causes negative consequences such as overload in the electric grid system triggering voltage collapse or, worse, damaging expensive extra-high voltage (EHV) power transformers. High voltage transformers are vulnerable to GIC, and almost all GMD-related issues are caused by the flow of GIC through the transformers. Since GIC is quasi-dc, it causes transformers to operate in the region of nonlinearity as it drives transformers to half-cycle saturation. Power transformers are designed to operate in the linear region of their magnetizing characteristics. When a power transformer is subjected to quasi dc current, the flow of zero sequence current into the transformer winding causes the shift in operating point. It results in a unidirectional shift in the flux as the dc flux adds to the ac flux in one-half cycle [1–4, 25–27], as shown in Figure 2.2. The large magnetizing current pulse as a result of unidirectional shift, as shown in orange in Figure 2.2 becomes a short duration pulse with high peak and increases the absorption of reactive power of the transformer [26–28]. Reactive power loss associated with half-cycle saturation is shunt loss, where the transformer behaves as a large reactive load. So, the power system sees a large demand in reactive power during the flow of GIC. This reactive power loss increase may reduce the system voltages to the point of encroaching secure voltage limits. Therefore, it can have a significant effect on reactive

power resources, reactive power margins, generator performance, and protective relaying. As a result, reactive power resources such as synchronous generator, shunt capacitor, static VAR compensator (SVC), and spinning reserve are exhausted, leading to a significant loss of reactive power support and voltage instability issues or large-scale voltage collapse [1–4, 28].

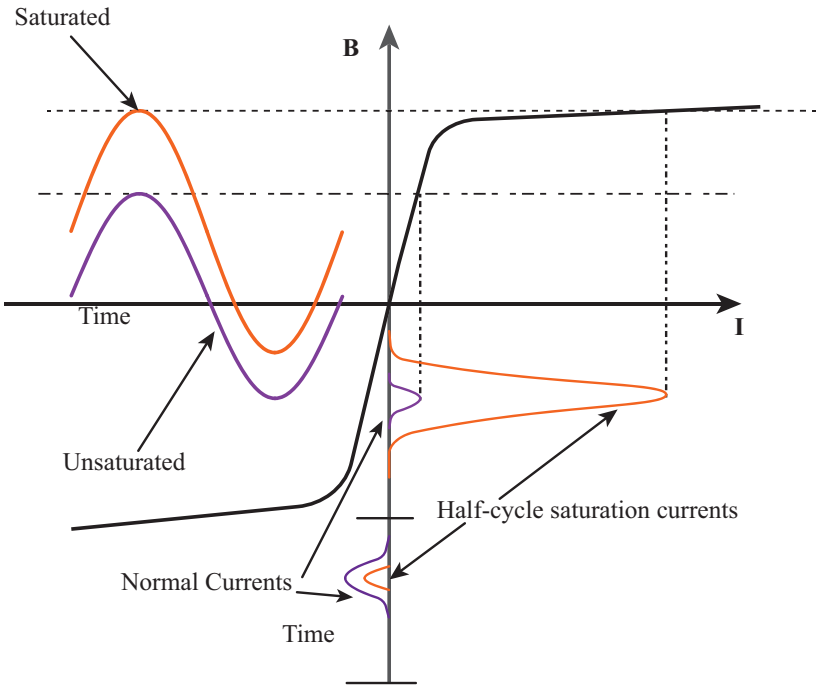

Figure 2.2: Half cycle saturation in transformer.

The large magnetizing current pulse generates odd, and even harmonics with significant magnitudes in the power system [3, 27, 29]. GIC-induced harmonics will flow to other devices in the system, depending on system topology and parameters. The elevated harmonic distortion causes protection and control devices to trip. Shunt capacitor banks used for reactive power support become low impedance paths for harmonic currents and can lead to tripping of the bank by relay protection schemes. Harmonic filters for SVCs create parallel

resonances that, if located at characteristic harmonic frequencies, can exacerbate voltage distortion issues and result in increased harmonics flow in these devices and tripping on protection. Harmonics can also cause the misoperation of electromechanical and solid-state relays, resulting in either nuisance operations or failure to operate when required. In the case of modern digital relays, where harmonic currents may be filtered, overcurrent protection of capacitor banks would become desensitized, thus reducing its effectiveness and potentially leading to capacitor bank damage [1].

The magnitude and duration of GIC affect the impacts it has on transformers and is a key consideration in determining the heating caused in transformers winding and structural parts [2, 3]. During GIC flow, high magnitudes of magnetization current pulses and associated current harmonics produce increased harmonic-rich stray flux. A greater share of flux leaks out beyond the core, inducing additional eddy currents in various parts of the core and winding assembly, including metallic structural parts, such as the tie plate and tank walls [30]. It would cause high winding circulating currents in transformers, causing overheating of power transformers which, if high and for a long duration, can subsequently reduce the life of transformers or even damage them. The consequence is additional heating at these locations, potentially causing gassing or simply resulting in accelerated aging of the cellulosic insulation due to thermal degradation. Heating of the tank walls due to eddy currents can also cause the interior paint to be peeled off, liberating contaminants into the oil. The result is that, at best, some of the useful life of the cellulosic insulation is lost, and, at worst, the unit is at a greater risk of incurring an imminent failure due to the gassing, causing dielectric strength to be compromised. Therefore, higher eddy current results in an increase in the hotspot temperature of transformers winding and structural parts and reduce the life span or cause the failure of the transformers [3, 24, 26, 27, 29–33]. The significant overheating of the

series connection of old (pre-1973) design shell form transformers at PSE&G during the 1989 GMD storm was an example of overheating of transformers attributed to GIC [1]. Depending on the transformer design and actual GIC magnitudes and duration, the tie-plate maximum temperatures could reach temperatures that would produce amounts of dissolved gas and have much consequence on the reliability of the transformer. Another consequence of the unidirectional flux density shift in the core is that significant increases in both core losses and core noise are experienced for the duration of the GMD event. The loss increase in the core results in an increase in the core hotspot temperature. While core noise increase is typically very noticeable onsite and is associated with higher magnitudes of core and tank vibrations, the rise in the core noise is only temporary and is limited to the duration of the GMD event [1]. As a whole, GIC due to GMD causes increased harmonic generation, excessive rise of transformers' hotspot temperature leading to thermal damage or significant loss of winding insulation life, increase in vibration and noise level, and malfunction of transmission line protection schemes [1, 34, 35]. IEEE standard C57.91-2011 [36] presents the hotspot temperature limit of transformers winding as $180\,^{\circ}C$ and tie-plate as $200\,^{\circ}C$ for short time emergency loading that should not be exceeded at either winding or structural hotspots on operating transformers to avoid undue aging of the winding insulation as well as to limit the risk of an imminent dielectric failure from gassing.

Necessary modeling details for the time domain simulation of GMD are included in different works of literature. To monitor the impacts of GMDs in power network, a system has been developed to provide real-time simulations of GIC flowing in the power system [37]. [25] presents an overview of modeling GMDs into the power flow to assess the impact on large-scale power systems focusing on the loss of reactive power support, potentially leading to a voltage collapse. [38] considers the chain of models: transforming surface magnetic

field disturbance to induce surface electric field through an electromagnetic transfer function and, then, induced surface electric field to GIC to model a realistic power topology and comparisons are made to transformer neutral current reference measurements provided by the American Transmission Company. [39] presents the system and model data of the IEEE 118 bus power system, including transmission lines, transformers, load, generations, GPS coordinates of substations, substation grounding impedance, and so on. These data can be incorporated in various simulations relating to GMD and GIC, although it does not represent the actual AEP grid. Several efforts have been made for thermal assessment of transformers due to GIC [24, 30, 40, 41]. [24] provides a system-wide transformer temperature analysis due to GIC-induced half-cycle saturation where it identifies potential overheated transformers in a GMD event and characterizes the relationship between the GIC and the transformer's temperature response.

2.3 Blocking Devices

Short-term and long-term remedies can be pursued to mitigate the adverse effects of GMD [1, 11, 42–45]. Several efforts in the literature have been reported to monitor [46, 47], control [48, 49], and mitigate [9, 50, 51] the impacts of GIC on power networks. Several actions can be taken to monitor the system stress due to the GIC flow in the power system, such as 1) monitoring unusual voltage and reactive power swings, 2) monitoring abnormal temperature rise/noise/dissolved gas in transformers, 3) preparing for unplanned capacitor bank/ static VAR compensators tripping, 4) monitor reactive power reserves, and 5) a reliable GIC forecasting. Many utilities rely on forecasts of geomagnetic activity to help them operate

during disturbances. The Canadian Geomagnetic Forecast Service, operated by Natural Resources Canada, has been in operation since 1974 and provides long-term and short-term forecasts for three latitude regions of Canada [13]. As a result of risk assessment, National Grid Company, the owner and operator of one of the world's largest privatized high-voltage electric power transmission systems in England and Wales at 400 kV and 275 kV, completed the installation of a Metatech Spacecast/Powercast space weather forecasting system in May 1999 [52] where operator displays for each forecast timescale would include alert and alarm status as well as forecast accuracy confidence levels. The space weather impact forecast would be displayed on a geographic system diagram with color bands indicating the forecast GIC impact, the total/zonal additional reactive power requirements to manage the system, and the time to forecast event impact [52]. Another solution would be re-configuring the power system, like removing affected transformers or transmission lines from service to redirect the flow of GIC [1] or re-dispatching generation and reactive power resources to stabilize system voltages [25]. However, removing transformers and transmission lines from the system during GIC flow can increase the effect on neighboring equipment, mainly transformers, as the GIC is redirected to them.

For smooth operation of substation and protection of ac systems, a long-term solution to eliminate the flow of GIC is the installation of GIC blocking devices (BDs) to eliminate or reduce the quasi-dc currents entering the transformer. A number of blocking devices have been studied in the past [5–8, 53]. Most of them are based on using a fairly large capacitor inserted into the transformer neutral, which may be expensive that costs $500K [54] and require significant space. GIC blocking devices such as inserting resistor or capacitor from neutral to ground connected to the grounded neutral of transformers eliminate or reduce GIC from entering through the transformers. Series capacitors can also be installed to block the

GIC flow in transmission lines [52, 55]. However, Series capacitor blockers are primarily used for series compensation of transmission lines but have a secondary effect of blocking dc current flow in transmission lines. They are considered less economical and limited by the impact on normal system operations, and thus blocking transformer neutral has been more popularly advocated [6]. In 1993, TransÉnergie commissioned IREQ to undertake the development of a dc current blocking device to be installed in transformer neutrals. The goal was for the device to be simple, economical, and suitable for integration at any transformer substation where the dc current flow needs to be limited [5]. DC blocking devices for the transformer neutrals were developed in [5] where it was essentially a capacitor inserted in series in the transformer neutral to block the dc current in the transformer. However, GIC blocking devices placed on the neutral of transformers block the GIC flow through the transformer but redirect its flow to the other neighboring transformers and can create problems in the transformers and power system and also exacerbate the voltage instability problem. Linear sensitivity analysis was done in [6] for the placement of BDs on the most sensitive transformers. [6] presents the GIC blocking device placement problem for actively mitigating the impact of solar activity on large power systems. The placement problem of multiple blocking devices was first considered by analytically quantifying the associated reactive power losses. A linear sensitivity analysis was provided for the case of blocking a single transformer, and it was observed that the effects of blocking transformer neutral currents are primarily local. The effectiveness of the proposed methods was shown using the 20-bus case and confirmed by the test results on a much larger case [6]. [53] proposes various risk reduction measures that could be adopted to ensure precise operation of neutral blocking devices (NBDs) for enhanced power system safety and reliability against dc. An ideal operational architecture consisting of control, communication, and physical layer has been proposed for the NBD installations in [53].

The BDs are fairly expensive to install and maintain, and the placement of BD on the neutral of one transformer can redirect the flow of GIC into other neighboring transformers as all power transformers are vulnerable and affected by GIC. Placement of BD in transformers neutral without enough research can potentially exacerbate voltage instability conditions and high temperature rise situation in other transformers and make the situation worse. So, the placement of BDs should be well optimized for effective and efficient operation and hence viewed as an optimization problem. The optimal placement was first done in [9] where the genetic algorithm from MATLAB optimization toolbox was approached in the IEEE 118-bus benchmark power system while ensuring the generator's real/reactive power and the system voltages are maintained within acceptable ranges. However, there has not been enough research on optimal placement of BDs that also considers and takes into account the thermal limit of the transformer hotspot. This thesis provides an approach to finding the optimal number of BDs and the transformers at which the BDs need to be placed to block the GIC and its harmful impacts on the power system. The optimal placement of BDs minimizes the number of installed BDs while ensuring a feasible power flow and voltage profile for the power grid and maintaining the hotspot temperature of every transformer in the grid.

Chapter 3

Power System Analysis Under GIC Conditions

3.1 Geomagnetically Induced Current Calculation

When GMD occurs, it disturbs the earth's magnetic field and induces quasi-dc geoelectric field E at earth's surface. This geoelectric field then induces dc voltage (voltage source) V_{dc} [56] in each phase of the transmission line between stations A and B, which is computed by integrating the geoelectric field along the route of the line [57] given by the equation

$$V_{\mathrm{dc}} = \oint E.\,dl \tag{3.1}$$

where E is the electric field at the location of transmission line, dl is the incremental length

of the transmission line, including direction, leading to the flow of GIC along transmission lines and through grounded transformers. GIC flow depends on both the magnitude and the direction of E. Assuming a constant geoelectric field in the geographic area of the transmission system, V_{dc} becomes independent of the path and only depends on the two ends of the transmission line. As a result, the incremental vector dl becomes L that represents length and direction of the lines connecting substations i and j [25, 57], and is given by equation

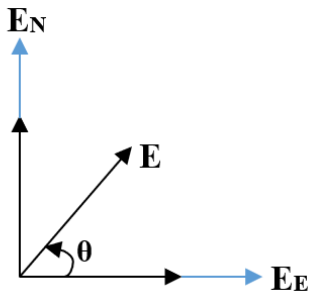

$$V_{\mathrm{dc}} = E.l = E_{\mathrm{N}} L_{\mathrm{N}} + E_{\mathrm{E}} L_{\mathrm{E}} \tag{3.2}$$

where $E_{\mathrm{N}}\,(V/km)$ is the northward geoelectric field, $E_{\mathrm{E}}\,(V/km)$ is the eastward geoelectric field, $L_{\mathrm{N}}\,(km)$ is the northward distance and $L_{\mathrm{E}}\,(km)$ is the eastward distance between the two endpoints of the transmission line. To obtain more accurate values (and to be consistent with substation latitudes and longitudes obtained from GPS measurements), it is necessary to take into account the non spherical shape of the Earth [57, 58]. The North-South distance, L_{N} is given by the equation:

$$L_{\mathrm{N}} = \frac{\pi}{180} M.\Delta lat \tag{3.3}$$

where M is the radius of curvature in the meridian plane and is described by (3.4) and Δlat is the difference in latitude (degrees) between the two substations A and B.

$$M = \frac{a(1-e^2)}{(1-e^2\sin^2\phi)^{1.5}} \tag{3.4}$$

where ϕ is defined in (3.5) as the average of the two latitudes of the two substations A and B, and a is the equatorial radius of the earth model whose value is 6378.137 km [57].

$$\phi = \frac{LatA + LatB}{2} \tag{3.5}$$

The East-West distance, L_{E} is given by the equation:

$$L_{\mathrm{E}} = \frac{\pi}{180} N \cos\phi . \Delta long \tag{3.6}$$

where N is the radius of curvature in the plane parallel to the latitude as defined by (3.7) and $\Delta long$ is the difference in longitude (degrees) between the two substations A and B [57].

$$N = \frac{a}{\sqrt{1-e^2\sin^2\phi}} \tag{3.7}$$

Due to the quasi-dc nature of GIC, the power system is represented as a dc network consisting of dc resistances of the transmission lines, transformer windings, and ground grid of the substations. So, the transformer dc model is needed for GIC calculation. The transformers are classified as autotransformers and step-up/down transformers. The dc models of autotransformers and step up/down transformers are represented in Figure 3.1

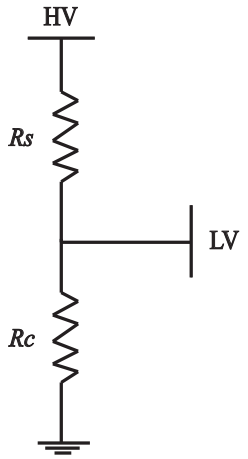

Figure 3.1: Representation of auto transformers in dc network model.

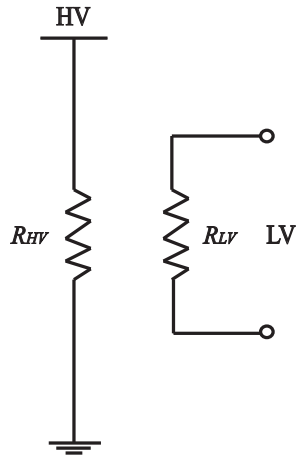

Figure 3.2: Representation of step up/down transformers in dc network model.

and Figure 3.2. In the case of auto-transformers, low voltage and high voltage terminals are electrically connected through the series winding with dc resistance R_S. The path to the ground is provided through the common winding with dc resistance R_C. But in the case of step-up/down transformers, high voltage (HV) and low voltage (LV) windings are separate, and only HV winding is modeled because LV side can be ungrounded or delta connected or connected to the local power system with insignificant induced GMD voltage. The voltage source V_{dc} is used as an input to the dc model of the network, and the resulting dc network can be solved using standard circuit analysis techniques to find GIC flowing in each line and each transformer. Nodal analysis is used to calculate GIC on each line and transformer because of its effectiveness in such networks. More details on GIC calculation can be found in [57, 59, 60]. After calculating GIC, the next step is calculating the additional reactive power loss of transformers associated with the GIC. The amount of this GIC related reactive power loss depends on the construction of transformer [9, 26, 61–64]. The reactive power loss

of the transformer as a result of the flow of GIC can be calculated by the equation

$$Q_{\mathrm{T}} = V_{p.u.} K I_{GIC} \tag{3.8}$$

where I_{GIC} is the GIC flowing in the transformer's winding $V_{p.u.}$ is the per unit voltage of transformer's terminal and K is a constant that depends on the transformer type and relates these quantities to transformer's reactive power loss [9, 61]. Under GMD, the calculated transformer's additional reactive power loss is represented as the reactive load connected to the transformer bus and the power flow analysis should be performed with the updated reactive power at the bus [9].

The main power flow equations are given by

$$P_i = \sum_{k=1}^{N} |V_i||V_k|(G_{ik}\cos\theta_{ik} + B_{ik}\sin\theta_{ik}) \tag{3.9}$$

$$Q_i = \sum_{k=1}^{N} |V_i||V_k|(G_{ik}\sin\theta_{ik} + B_{ik}\cos\theta_{ik} \tag{3.10}$$

where P_i is the net real power and Q_i is the net reactive power injected at bus i, G_{ik} is the real part and B_{ik} is the imaginary part of the element $ikth$ in the bus admittance matrix Y_{Bus}. At the event of GMD, transformers additional reactive losses Q_T during the flow of GIC should be included as

$$Q_{i,new} = Q_i - Q_T \tag{3.11}$$

The power flow equations are then solved using the updated reactive power from 3.11.

3.2 Transformer Thermal Assessment

The injection of GIC into the system transformers with grounded neutral saturates the transformer and 1) increases its reactive power demand, 2) turns the transformer into a harmonic current source, and 3) causes hotspot overheating in the transformer [51, 65, 66]. The much higher magnetizing current resulting from the addition of unidirectional dc flux in the core, and the nature of its wave – shape, produce correspondingly higher magnitudes of leakage flux that is also rich in harmonics. This results in appreciably higher eddy and circulating current losses in the windings as well as the structural parts of the transformer, degrading insulation resulting in the accelerated aging of the insulation [67–70], gassing [71] and liberating contamination into the oil due to peeling of interior paint [12]. The advanced transformer model of [62, 63], which is the most accurate transformer model for GIC studies [63, 64], has been simulated in the time-domain, and the harmonic characteristics of each core construction have been obtained as a function of the applied GIC, and the system voltage in [51].

[12] presents the calculation of transformers winding and structural parts temperatures when subjected to several levels of step dc currents (20, 30, and 50 Amps / Phase) for fully loaded transformers (asymptotic value of step response). For the winding hotspot temperature calculation, the dc was subjected for 30 minutes, and only about $12\,^{\circ}C$ increase was observed, which was an insignificant rise in hotspot temperature even after being subjected to 50 Amps dc for 30 minutes. For the calculation of tie plate hotspot temperature of transformers, different values of dc was applied for 120 minutes continuously. The magnitude of this temperature rise depends on the core construction, the operating / design flux density, and the magnitude of dc current flowing through the windings. Once the core flux density reaches

close to the saturation flux density level of the core steel, there will be spillage of the core flux outside the core. This results in additional flux linkages to the structural parts, such as tie plates, yoke clamps, tank walls, tank cover, tank bottom, etc. [12]. The rise in hotspot temperature was still insignificant after being continuously subjected to 50 Amps for 120 minutes and only was about 32 $^{\circ}C$.

A thermal equivalent circuit of transformers based on a basic heat transfer model is suggested in [30, 40]. Field test research on top oil temperature rise and heating parameter estimation is reported in [71, 72]. A transformer heating assessment is presented in [41] to describe thermal models for hotspot temperature rise in transformers. Thermal impacts of dc currents on power transformers (winding and metallic parts) are investigated in [73]. [74] develop a thermo-electrical model using finite element methods to evaluate temperature distributions in the windings. [24] develops, for the first time, a systematic framework to assess the thermal response of transformers during GMD events: (i) analyze the time-varying temperature behavior in normal operating conditions (when all transformers are fully functioning), (ii) contingency scenarios (when a transformer is expected to be thermally damaged), and determine the characteristics of the most thermally vulnerable transformers in the power system. [75] provides transformer thermal impact assessment based on two types of GMD events. Two kinds of GMD Vulnerability Assessments are used to evaluate the potential impacts of GMD events on the Bulk Electric System in [75]. The benchmark GMD Vulnerability Assessment is based on the benchmark GMD event, where the benchmark GMD event is derived from spatially-averaged geoelectric field values to address potential wide-area effects that could be caused by a severe 1-in-100 year GMD event [76, 77] and the supplemental GMD Vulnerability Assessment is based on the supplemental GMD event, is used by entities to evaluate risks that localized peaks in the geomagnetic field during

a severe GMD event that could potentially affect the reliable operation of the bulk power system. Transformers must undergo a thermal impact assessment if the maximum effective geomagnetically induced current (GIC) in the transformer is equal to or greater than 75 A per phase for the benchmark GMD event and 85 A per phase for the supplemental GMD event [75]. [30] uses the electric field associated with an extreme GMD event to estimate internal hotspot temperatures on a real-time basis during an ongoing GMD event, using response functions fitted to particular thermal step-response data either measured or supplied by the manufacturer. The method is based on fitting a closed form analytical function to the calculated or measured thermal response of a particular transformer design, typically provided by the manufacturer, at the hotspot location of the transformer to a step dc current excitation [3, 12]. This fitted function can then be used to simulate the hotspot temperature profile for transformers. The transformer spot-heating is taken into account based on the steady-state temperature rise characteristics shown in [30], noting that higher temperature rises have also been reported in the literature [30]. Assuming the full-load temperature rises prior to the GMD event, the total temperature due to GIC is checked in the proposed mitigation approach to be below the maximum standard permissible values [30]. An accurate thermal transformer model for estimating the hotspot heating in the transformer during GMDs has been developed in [78], which is generic and does not require detailed transformer data.

IEEE Standard C57.91-2011 [36] provides an IEEE guide for the maximum temperature limit that should not be exceeded on the hotspot of transformer windings and other structural parts to avoid the accelerated aging of insulation as well as to avoid the dielectric failure at windings and structural hotspots due to gassing. Suggested limits for each hotspot temperature of transformer windings and other metallic structures are presented in Table 3.1 and are

assumed to be relevant for GIC. Normal life expectancy loading is considered risk-free but the other types of loading have risk associated to them. The maximum temperature limit for the windings of the transformer at full load is 180 $^{\circ}C$ and that of structural parts such as tie plate is 200 $^{\circ}C$, top oil temperature being 110 $^{\circ}C$. If the transformer temperature exceeds these limits, it can cause the insulation of transformers to fail and damage the expensive high voltage transformers. So, it is crucial to maintain the hotspot temperature of transformer windings and tie plates within these maximum limits. The risks associated with exceeding these thresholds also vary with individual units' mechanical and dielectric condition, which, in turn, depends on the operating history [79].

Table 3.1: Maximum temperature limits suggested in IEEE C57.91 2011

	Normal life expectancy loading	Planned loading beyond nameplate rating	Long time emergency loading	Short time emergency loading
Insulated conductor hottest spot temperature ($^{\circ}C$)	120	130	140	180
Other metallic hottest spot temperature ($^{\circ}C$)	140	150	160	200
Top oil temperature ($^{\circ}C$)	105	110	110	110

In this thesis, the GMD event is taken from the recorded 1989 Hydro Quebec event, and temperature rises are simulated for both winding and tie-plate of transformers with time constants 2.5 min and 2.9718 min, respectively. Based on the winding and tie-plate temperature rise, the transformers are assumed to be repaired or replaced if the hotspot temperature exceeds the maximum limit. If the hotspot temperature is higher than 1.5 times the maximum temperature limit, it is assumed to be replaced; otherwise, it is assumed to be repaired. The cost of replacing transformers is \$6000/MVA, and the cost of repair of

transformers is $4000/MVA [80].

3.3 Study System

The demonstration of detrimental effects of GIC and the optimization for BD placement to eliminate the adverse effects is done in IEEE-118 bus standard test system [39]. This test system is deemed suitable for this study because of the reason that most of the necessary information are readily available such as:

- the substations coordinates and coordinates of the ends of transmission lines are required. Their latitude and longitude are available, if not it can be found using maps and online tools using the name of substations and cities where they are located because the test system was developed based on a portion of the American Electric Power(AEP) power grid (in the Midwest U.S.),
- network configuration and parameters such as resistances and reactances of the transmission lines and transformers, and load and generation data are readily available [9, 39, 81].

3.3.1 Substation Data

The geographical view of substation locations is shown in Figure 3.3 on the map of United States of America. The IEEE-118-bus system spans the states of Indiana, Ohio, West Virginia, Virginia, Kentucky, and North Carolina. The GPS coordinates of the substation locations

(latitude and longitude) are presented in Table 3.2 and the names of substations and the respective substation grounding resistance are presented in Table 3.3.

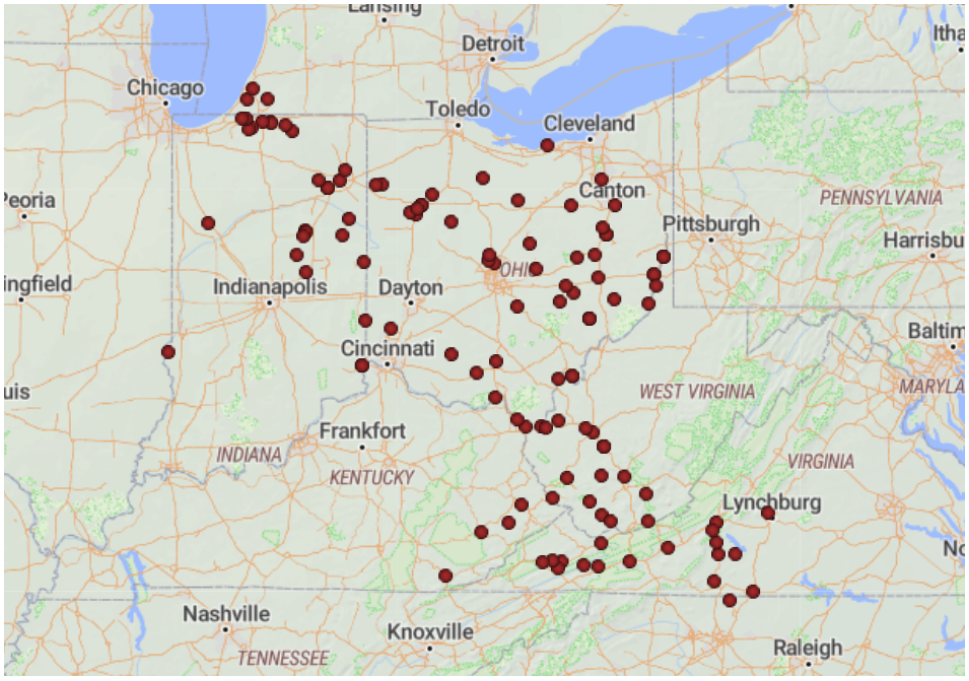

Figure 3.3: IEEE 118-bus standard system overlaying the map of the U.S.

3.3.2 Transmission Line Data

The total number of lines in the 118-bus test system is 177 [39]. The transmission line data is presented in Table 3.4 with their respective bus number. Other data required for the simulation are the admittance and line length which are presented in the Table 3.4.

Table 3.2: GPS coordinates of Substations

Bus	Latitude (°)	Longitude (°)	Bus	Latitude (°)	Longitude (°)	Bus	Latitude (°)	Longitude (°)
1	42.022008	-86.387215	41	41.086597	-83.171997	81	38.196711	-81.480250
2	41.914541	-86.182251	42	40.850863	-82.681363	82	37.850640	-81.995064
3	41.910453	-86.467896	43	40.624376	-83.614197	83	37.629006	-82.197474
4	41.710342	-86.539307	44	40.392058	-82.516594	84	37.553832	-82.631264
5	41.706674	-86.483862	45	40.122716	-82.426300	85	37.354330	-82.810822
6	41.597986	-86.445923	46	39.718807	-82.691345	86	37.249461	-83.193283
7	41.616469	-86.403008	47	39.771603	-82.095337	87	36.762438	-83.692653
8	41.706674	-86.483862	48	39.941117	-82.011655	88	36.913606	-82.337070
9	40.609782	-87.011719	49	39.865158	-81.904034	89	36.932778	-82.198611
10	39.227333	-87.570961	50	40.029455	-81.558380	90	36.847809	-82.121367
11	41.677015	-86.252289	51	40.272322	-81.605759	91	36.922555	-82.070591
12	41.665088	-86.132140	52	40.243502	-81.856041	92	36.881268	-81.762142
13	41.642131	-85.930939	53	40.797697	-81.937408	93	37.125286	-81.518555
14	41.579498	-85.836868	54	41.072104	-81.513062	94	37.371590	-81.385516
15	41.170632	-85.096655	55	40.799138	-81.325396	95	37.439474	-81.508612
16	41.063777	-85.467300	56	40.562330	-81.496582	96	37.589264	-81.679157
17	40.983705	-85.342592	57	40.490043	-81.445427	97	37.876389	-81.514606
18	41.060957	-85.172408	58	40.490043	-81.445427	98	37.865390	-81.193684
19	41.014555	-84.666824	59	40.252500	-80.645556	99	37.673948	-80.888985
20	40.654898	-85.044858	60	39.942384	-80.749512	100	37.371389	-80.862222
21	40.480871	-85.136271	61	40.062308	-80.779724	101	36.922633	-81.119144
22	40.196391	-84.836187	62	39.749389	-80.854778	102	36.866987	-81.559971
23	39.567687	-84.814453	63	40.252500	-80.645556	103	37.074833	-80.584466
24	39.480991	-84.457226	64	40.062308	-80.779724	104	37.005112	-79.643772
25	39.081507	-84.861495	65	39.588658	-81.682026	105	37.270228	-79.961460
26	39.081507	-84.861495	66	39.588658	-81.682026	106	37.357059	-79.906625
27	40.087173	-85.644216	67	39.796766	-81.335950	107	37.463571	-79.185785
28	40.271203	-85.774719	68	38.967194	-81.921389	108	37.135231	-79.906823
29	40.472024	-85.682373	69	38.967194	-81.921389	109	37.003889	-79.879460
30	40.983705	-85.342592	70	38.733732	-82.997589	110	36.700334	-79.938897
31	40.515952	-85.644024	71	39.001043	-83.259190	111	36.486200	-79.720800
32	40.271372	-83.081821	72	39.202573	-83.611506	112	36.585200	-79.394180
33	41.019283	-84.580994	73	39.126509	-82.986133	113	40.530651	-85.653395
34	40.762827	-84.087725	74	38.492630	-82.690150	114	40.211490	-83.092430
35	40.722283	-84.186859	75	38.413800	-82.574164	115	40.181841	-83.011368
36	40.701428	-84.107544	76	38.480111	-82.115696	116	38.935395	-82.116390
37	40.800649	-84.029870	77	38.402801	-82.290856	117	41.675968	-86.141166
38	40.800649	-84.029870	78	38.396747	-81.733692	118	38.417642	-82.355112
39	40.912651	-83.880775	79	38.351978	-81.634194			
40	41.430002	-82.269469	80	38.196711	-81.480250			

Table 3.3: Name of Substations, Substation grounding resistance

Substation	$R_g(\Omega)$	Substation	$R_g(\Omega)$	Substation	$R_g(\Omega)$
Riversde	0.1	Howard	0.1	BetsyLne	0.1
Pokagon	0.1	S.Kenton	0.1	BeaverCk	0.1
HickryCk	0.1	WMVernon	0.1	Hazard	0.1
NwCarlsl	0.1	N.Newark	0.1	Pinevlle	0.1
Olive	0.1	W.Lancst	0.1	Fremont	0.1
Kankakee	0.1	Crooksvl	0.1	ClinchRv	0.1
JacksnRd	0.1	Zanesvll	0.1	Holston	0.1
Bequine	0.1	Philo	0.1	HolstonT	0.1
Breed	0.1	WCambrdg	0.1	Saltvlle	0.1
SouthBnd	0.1	Newcmrst	0.1	Tazewell	0.1
TwinBrch	0.1	SCoshoct	0.1	Switchbk	0.1
Concord	0.1	Wooster	0.1	Carswell	0.1
GoshenJt	0.1	Torrey	0.1	Baileysv	0.1
FtWayne	0.1	Wagenhls	0.1	Sundial	0.1
N.E.	0.1	Sunnysde	0.1	Bradley	0.1
Sorenson	0.1	WNwPhil1	0.1	Hinton	0.1
McKinley	0.1	WNwPhil2	0.1	GlenLyn	0.1
Lincoln	0.1	Tidd	0.1	Wythe	0.1
Adams	0.1	SWKammer	0.1	Smythe	0.1
Jay	0.1	Kammer	0.1	Claytor	0.1
Randolph	0.1	Natrium	0.1	Hancock	0.1
CollCrnr	0.1	Muskngum	0.1	Roanoke	0.1
Trenton	0.1	Summerfl	0.1	Cloverdl	0.1
TannrsCk	0.1	Sporn	0.1	Reusens	0.1
Madison	0.1	Portsmth	0.1	Blaine	0.1
Mullin	0.1	NPortsmt	0.1	Franklin	0.1
Grant	0.1	Hillsbro	0.1	Fieldale	0.1
DeerCrk	0.1	Sargents	0.1	DanRiver	0.1
Delaware	0.1	Bellefnt	0.1	Danville	0.1
Haviland	0.1	SthPoint	0.1	DeerCrk2	0.1
Rockhill	0.1	Darrah	0.1	WMedford	0.1
WestLima	0.1	Turner	0.1	Medford	0.1
Sterling	0.1	Chemical	0.1	KygerCrk	0.1
EastLima	0.1	CapitlHl	0.1	Corey	0.1
NwLibrty	0.1	Kanawha	0.1	WHuntngd	0.1
WestEnd	0.1	Logan	0.1		
S.Tiffin	0.1	Sprigg	0.1		

Table 3.4: Transmission lines data

From	To	y_line	Line length (km)	From	To	y_line	Line length (km)	From	To	y_line	Line length (km)	From	To	y_line	Line length (km)
1	2	0.1993	100	34	36	0.6935	100	64	65	0.3592	100	92	94	0.1255	100
1	3	0.4682	100	34	37	2.3585	100	49	66	0.3355	100	93	94	0.2708	100
4	5	3.4364	100	37	39	0.1881	100	49	66	0.3355	100	94	95	0.4575	100
3	5	0.2506	100	37	40	0.1018	100	62	66	0.1253	100	80	96	0.1696	100
5	6	0.5074	100	30	38	0.2082	100	62	67	0.2341	100	82	96	0.3727	100
6	7	1.3158	100	39	40	0.3282	100	66	67	0.2696	100	94	96	0.2245	100
8	9	0.3960	100	40	41	0.4165	100	65	68	0.7003	100	80	97	0.3300	100
9	10	0.3745	100	40	42	0.1088	100	47	69	0.0715	100	80	98	0.2537	100
4	11	0.2889	100	41	42	0.1473	100	49	69	0.0613	100	80	99	0.1330	100
5	11	0.2974	100	43	44	0.0993	100	69	70	0.2013	100	92	100	0.0932	100
11	12	1.0152	100	34	43	0.1462	100	24	70	2.7322	100	94	100	0.3392	100
2	12	0.3229	100	44	45	0.2696	100	70	71	0.6845	100	95	96	0.3531	100
3	12	0.1248	100	45	46	0.1510	100	24	72	0.1237	100	96	97	0.3490	100
7	12	0.7008	100	46	47	0.1589	100	71	72	0.1354	100	98	100	0.1521	100
11	13	0.2714	100	46	48	0.1005	100	71	73	0.6974	100	99	100	0.3355	100
12	14	0.2809	100	47	49	0.3162	100	70	74	0.1506	100	100	101	0.2180	100
13	15	0.0812	100	42	49	0.0845	100	70	75	0.1411	100	92	102	0.4909	100
14	15	0.1015	100	42	49	0.0845	100	69	75	0.1491	100	101	102	0.2455	100
12	16	0.2848	100	45	49	0.0883	100	74	75	0.4909	100	100	103	0.3774	100
15	17	0.4575	100	48	49	0.3374	100	76	77	0.1360	100	100	104	0.1339	100
16	17	0.1330	100	49	50	0.2261	100	69	77	0.1954	100	103	104	0.1296	100
17	18	0.4909	100	49	51	0.1243	100	75	77	0.1005	100	103	105	0.1129	100
18	19	0.5397	100	51	52	0.2974	100	77	78	1.6051	100	100	106	0.0998	100
19	20	0.2396	100	52	53	0.1491	100	78	79	1.1062	100	104	105	0.6075	100
15	19	0.5033	100	53	54	0.2296	100	77	80	0.3552	100	105	106	0.4314	100
20	21	0.3300	100	49	54	0.0827	100	77	80	0.2054	100	105	107	0.1139	100
21	22	0.2889	100	49	54	0.0695	100	79	80	0.3871	100	105	108	0.2314	100
22	23	0.1766	100	54	55	0.3573	100	68	81	0.5522	100	106	107	0.1139	100
23	24	0.4472	100	54	56	2.1978	100	77	82	0.2026	100	108	109	0.5750	100
23	25	0.3871	100	55	56	1.2376	100	82	83	0.5391	100	103	110	0.1546	100
25	27	0.1899	100	56	57	0.1761	100	83	84	0.0966	100	109	110	0.2172	100
27	28	0.3157	100	50	57	0.1274	100	83	85	0.1404	100	110	111	0.2745	100
28	29	0.2548	100	56	58	0.1761	100	84	85	0.2000	100	110	112	0.2445	100
8	30	0.2242	100	51	58	0.2368	100	85	86	0.1725	100	17	113	0.6614	100
26	30	0.1209	100	54	59	0.1200	100	86	87	0.2135	100	32	113	0.0982	100
17	31	0.1274	100	56	59	0.0732	100	85	88	0.3019	100	32	114	0.4472	100
29	31	0.5593	100	56	59	0.0752	100	85	89	0.2527	100	27	115	0.3682	100
23	32	0.1905	100	55	59	0.1274	100	88	89	0.4344	100	114	115	2.6247	100
31	32	0.2026	100	59	60	0.1905	100	89	90	0.1166	100	68	116	2.8409	100
27	32	0.2637	100	59	61	0.1841	100	89	90	0.2537	100	12	117	0.1836	100
15	33	0.1589	100	60	61	2.2883	100	90	91	0.2378	100	75	118	0.4165	100
19	34	0.0803	100	60	62	0.4909	100	89	92	0.6101	100	76	118	0.3682	100
35	36	2.6954	100	61	62	0.7326	100	89	92	0.1537	100				
35	37	0.5488	100	63	64	0.5618	100	91	92	0.1560	100				
33	37	0.1455	100	38	65	0.1072	100	92	93	0.2341	100				

3.3.3 Transformers Data

The total number of transformers in the 118-bus test system is 162 with 9 autotransformers that connects 345 kV buses to 138 kV buses and the rest are step up/down transformers. The rated MVA of transformers is as provided in [81] and is essential in calculating the reactive power loss and terminal voltage during the flow of GIC. The data for auto transformers is provided in Table 3.5 with their respective primary side and secondary side bus number, Y of their common winding and series winding and their rated MVA. Table 3.6 presents the data for generator transformers with the bus to which they are connected, Y and their respective rated MVA. Similarly, Table 3.7 presents the data of load transformers with the bus number to which they are connected, Y and their respective rated MVA.

Table 3.5: Auto transformer data

Transformer number	Primary side bus	Secondary side bus	Y(common winding)	Y(series winding)	S(MVA)
1	8	5	5	3.33	700
2	26	25	5	3.33	220
3	30	17	5	3.33	475
4	38	37	5	3.33	500
5	63	59	5	3.33	330
6	64	61	5	3.33	90
7	65	66	5	3.33	220
8	68	69	5	3.33	650
9	81	80	5	3.33	165

For the simulation, the geoelectric field derived from the 1989 Hydro Quebec event is used and scaled from $E = 1\,V/km$ to $E = 8\,V/km$. The data from the event was recorded for 1440 minutes. Therefore, all the data and results are based on the data from that time

frame. The minimum permissible voltage is assumed to be $0.94\,p.u.$ The blocker to be placed is represented by a very high resistance in the calculation of GIC. The Q_{max} to P_{max} ratio is assumed to be 0.55 where the associate P_{max} is taken from [81]. The top oil temperature of transformer is taken as $105\,°C$.

Table 3.6: Generator transformers data

Transformer number	Bus	Y	S(MVA)	Transformer number	Bus	Y	S(MVA)	Transformer number	Bus	Y	S(MVA)
10	1	2.50	125	28	42	2.50	125	46	80	2.50	750
11	4	2.50	125	29	46	2.50	150	47	85	2.50	125
12	6	2.50	125	30	49	2.50	350	48	87	2.50	125
13	8	2.50	125	31	54	2.50	200	49	89	2.50	1000
14	10	2.50	750	32	55	2.50	125	50	90	2.50	125
15	12	2.50	250	33	56	2.50	125	51	91	2.50	125
16	15	2.50	125	34	59	2.50	350	52	92	2.50	125
17	18	2.50	125	35	61	2.50	350	53	99	2.50	125
18	19	2.50	125	36	62	2.50	125	54	100	2.50	500
19	24	2.50	125	37	65	2.50	600	55	103	2.50	200
20	25	2.50	500	38	66	2.50	600	56	104	2.50	125
21	26	2.50	500	39	69	2.50	1000	57	105	2.50	125
22	27	2.50	125	40	70	2.50	125	58	107	2.50	125
23	31	2.50	125	41	72	2.50	125	59	110	2.50	125
24	32	2.50	125	42	73	2.50	125	60	111	2.50	150
25	34	2.50	125	43	74	2.50	125	61	112	2.50	125
26	36	2.50	125	44	76	2.50	125	62	113	2.50	125
27	40	2.50	125	45	77	2.50	125	63	116	2.50	125

Table 3.7: Load transformers data

Transformer number	Bus	Y	S(MVA)	Transformer number	Bus	Y	S(MVA)	Transformer number	Bus	Y	S(MVA)
64	1	2.50	100	97	42	2.50	150	130	83	2.50	37.5
65	2	2.50	37.5	98	43	2.50	30	131	84	2.50	20
66	3	2.50	80	99	44	2.50	30	132	85	2.50	50
67	4	2.50	80	100	45	2.50	100	133	86	2.50	37.5
68	6	2.50	100	101	46	2.50	50	134	88	2.50	80
69	7	2.50	30	102	47	2.50	60	135	90	2.50	350
70	8	2.50	50	103	48	2.50	37.5	136	91	2.50	15
71	11	2.50	125	104	49	2.50	150	137	92	2.50	100
72	12	2.50	80	105	50	2.50	30	138	93	2.50	25
73	13	2.50	60	106	51	2.50	30	139	94	2.50	60
74	14	2.50	25	107	52	2.50	30	140	95	2.50	80
75	15	2.50	150	108	53	2.50	40	141	96	2.50	80
76	16	2.50	50	109	54	2.50	200	142	97	2.50	30
77	17	2.50	20	110	55	2.50	125	143	98	2.50	60
78	18	2.50	125	111	56	2.50	150	144	99	2.50	80
79	19	2.50	80	112	57	2.50	20	145	100	2.50	80
80	20	2.50	30	113	58	2.50	20	146	101	2.50	40
81	21	2.50	25	114	59	2.50	500	147	102	2.50	15
82	22	2.50	20	115	60	2.50	125	148	103	2.50	50
83	23	2.50	15	116	62	2.50	125	149	104	2.50	80
84	24	2.50	20	117	66	2.50	80	150	105	2.50	80
85	27	2.50	125	118	67	2.50	50	151	106	2.50	80
86	28	2.50	30	119	70	2.50	125	152	107	2.50	80
87	29	2.50	37.5	120	72	2.50	20	153	108	2.50	15
88	31	2.50	80	121	73	2.50	15	154	109	2.50	15
89	32	2.50	100	122	74	2.50	125	155	110	2.50	80
90	33	2.50	37.5	123	75	2.50	80	156	112	2.50	125
91	34	2.50	100	124	76	2.50	125	157	113	2.50	15
92	35	2.50	60	125	77	2.50	125	158	114	2.50	15
93	36	2.50	60	126	78	2.50	125	159	115	2.50	37.5
94	39	2.50	50	127	79	2.50	80	160	116	2.50	350
95	40	2.50	125	128	80	2.50	200	161	117	2.50	37.5
96	41	2.50	60	129	82	2.50	100	162	118	2.50	60

Chapter 4

Optimization Approach for GIC Blocking Device Placement

Installing GIC blocking devices (BD) at the neutral of power transformers is a long-term solution. After calculating the reactive power loss of transformers associated with the flow of GIC, bus voltages, and calculating the hotspot temperature rise of transformer tie-plate and windings, the most vulnerable transformers are identified based on their temperature rise and BDs are placed on the neutral of these transformers. But just placing BDs on the most vulnerable transformer is not an effective solution as it does not guarantee the normal operation of power system and is not an optimal solution. The BD placement problem should be viewed as an optimization problem [9, 10, 51] because of the following reasons:

- blocking devices are expensive which cost half a million dollars [54],
- and placing BD on one transformer redirects the flow of GIC to the neighboring

transformers and may well exacerbate the temperature rise and voltage instability situation.

4.1 Problem Formulation

The placement of BD should be well optimized to ensure the constraints are not violated and the operation of the power system is normal. The two main constraints this thesis considers are voltage constraint and transformer hotspot temperature constraint. The bus voltages should be above the minimum permissible limit, and the transformers' hotspot temperature should be below the maximum limit for both transformer tie-plate and winding. The following optimization formulation can be proposed:

$$\underset{x}{\text{minimize}} \quad C(x) = \sum_{i=1}^{n} c.x_i$$

$$\text{Subject to } V_{\text{i}} \geq V_{\text{min}}, i = 1, 2, ..., m$$

$$T_{\text{rise}_{\text{n}}} \leq T_{\text{max}}, n = 1, 2, ..., n$$

where, $V_{min} = 0.94\, p.u.,\ T_{\text{max}} = 200\ ^{\circ}C$ for tie-plate and $T_{\text{max}} = 180\ ^{\circ}C$ for winding.

Where $C(x)$ is the cost function, c is the cost of a BD, n is the total number of candidate transformers for BD installation, x is an n-dimensional binary vector representing the solution of the problem, x_{i} is the ith element of x indicating whether BD is installed on the ith transformer, whose value is either 0 or 1, V_{i} is the voltage of the ith bus, V_{min} is the minimum

permissible voltage level which is $0.94\,p.u.$, and m is the number of system buses.

The optimization is performed in such a way that the most vulnerable transformers with high hotspot temperature rise are identified, BDs are placed at the neutral of those transformers, the bus voltage violations are identified after placing BDs and insuring that the maximum rise in hotspot temperature of transformers is not more than the maximum limit T_{max}. To maintain the system bus voltage above the minimum permissible voltage V_{min}, the change in load can be done, and cost can be calculated in loss of load because it can be cheaper than placing extra BDs to maintain the voltage profile. Sometimes, decreasing total load could make the voltage profile even worse, so, in this case, BD should be placed in specific additional transformers to maintain the voltage profile. This way, the number of BDs and the total cost can be minimized.

The optimization approach ensures that the number of BDs and the total cost are as minimum as possible and none of the constraints are violated. The problem is formulated for different levels of E ranging from $E = 1\,V/km$ to $E = 8\,V/km$. For a given $E\,(V/km)$, GIC flow is calculated in each line and each transformer. Power flow analysis is done, and the voltage violation is checked at each bus. The hotspot temperature rise of each transformer is calculated for the given E. If there is no voltage violation and the transformers' hotspot temperature rise does not exceed the maximum limit, no BD is needed to be installed. If voltage violation occurs or the hotspot temperature rise of the transformer exceeds the maximum limit, then BD needs to be installed in certain transformers. The optimization algorithm places BDs on certain transformers, the voltage violation and hotspot temperature rise are rechecked after placing BDs and made sure these constraints are not violated. So, the placement is optimized without violating any of the voltage and temperature constraints.

The constrained optimization problem can be changed to an unconstrained optimization problem by adding penalties for each constraint violated.

$$F(x) = C(x) + P1 + P2 \tag{4.1}$$

where $P1$ and $P2$ are penalties for each of the bus voltage and transformer temperature rise constraint violation and are given by the following equations.

$$\text{P1} = \begin{cases} 0 & \text{if } V_{\text{i}} \geq V_{\min}, i = 1, ..., m \\ 1000 & \text{else} \end{cases}$$

$$\text{P2} = \begin{cases} 0 & \text{if } T_{\text{i}} \leq T_{\max}, i = 1, ..., n \\ 4000 & \text{if } T_{\max} \leq T_{\text{i}} \leq 1.5T_{\max} \\ 6000 & \text{else} \end{cases}$$

Thus, the voltage and temperature limit constraints are handled by adding large penalty values to the cost function for each constraint violation. The penalty value for voltage violation is taken in such a way that it is an enough large value added in the cost function and the penalty value for transformer temperature limit constraint violation is taken differently based on either the transformer is needed to be repaired or replaced. The penalty values added to the cost function are based on the cost of the repair or replacement of transformers, as described in the chapter 3. The optimization process is also described in the flowchart in Figure 4.1.

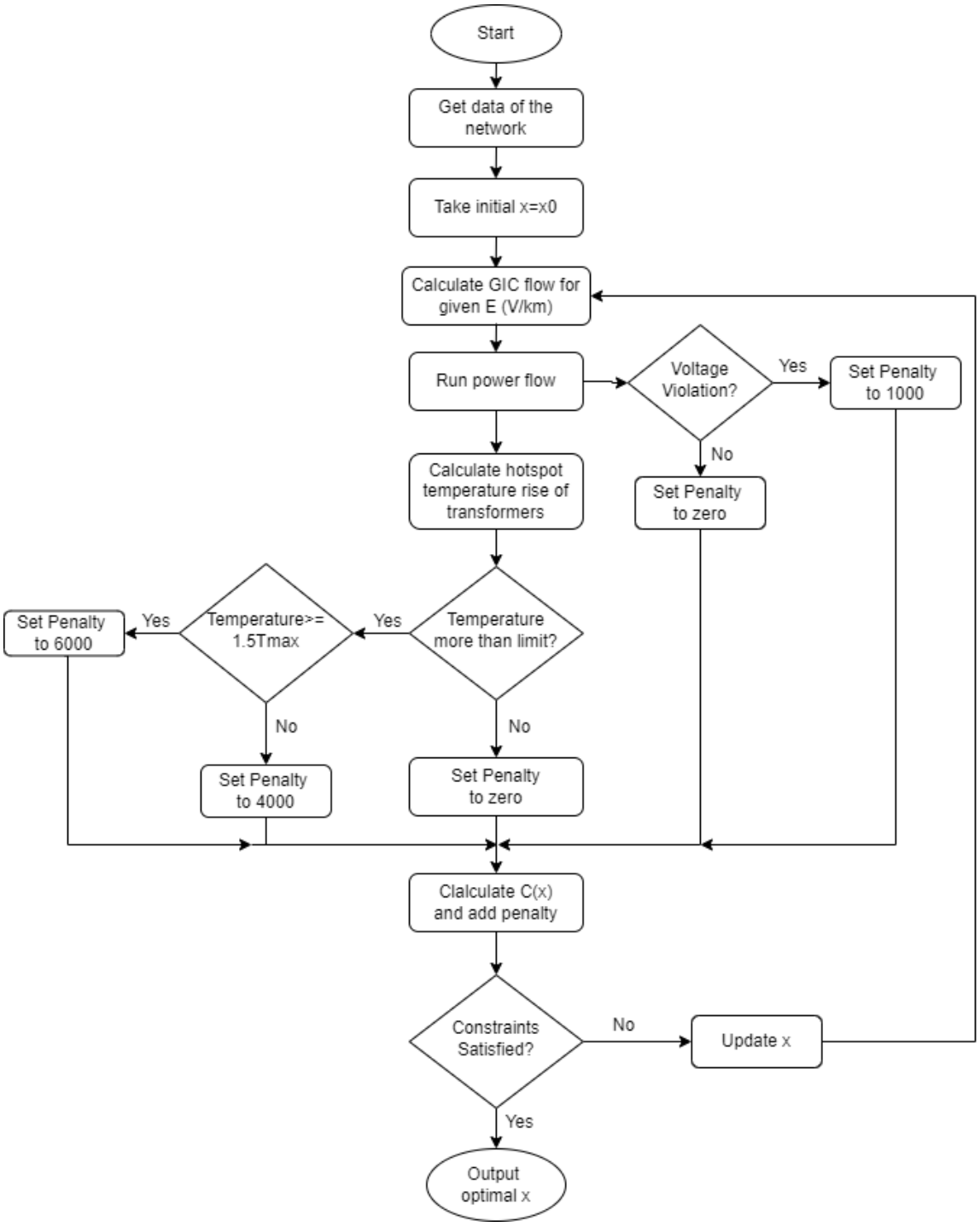

Figure 4.1: Optimal BD placement flowchart

4.2 Optimization Solvers

Depending on the type of problem, whether a local or global solution is required, a solver must be selected. The optimization problem of GIC BD placement requires a global minimum as the number of BDs should be as minimum as possible without violating any constraints. A global minimum is a point where the function value is smaller than or equal to the value at all other feasible points. Choosing a solver based on problem characteristics and the type of solution wanted is the next step after determining the kind of problem. Several solvers are available in the MATLAB optimization toolbox, such as GlobalSearch, MultiStart, Genetic Algorithm, Particleswarm, Simulated Annealing Algorithm, Patternsearch, and Surrogate Optimization [82].

The characteristics of the solvers in the MATLAB optimization toolbox are presented in Table. 4.1. Solvers can fail to converge to any solution when started far from a local minimum. When started near a local minimum, gradient-based solvers quickly converge to a local minimum for smooth problems. Patternsearch provably converges for a wide range of problems, but the convergence is slower than gradient-based solvers. Both genetic algorithm and particleswarm can fail to converge in a reasonable amount of time for some problems, although they are often effective. However, surrogate optimization and simulated annealing are proven to converge to the global optimum. Simulated annealing is usually the least efficient solver. Solvers iterate to find solutions. The steps in the iteration are iterates. Some solvers have deterministic iterates. Others use random numbers and have stochastic iterates. Some solvers use estimated or user-supplied derivatives in calculating the iterates. Other solvers do not use or estimate derivatives but use only objective and constraint function values. Most solvers require to provide a starting point for the optimization in order to obtain

Table 4.1: Solver Characteristics

Solver	Convergence	Characteristics
GlobalSearch	Fast convergence to local optima	Deterministic iterates
		Gradient-based
		Automatic stochastic start points
		Removes many start points heuristically
MultiStart	Fast convergence to local optima	Deterministic iterates
		Can run in parallel
		Gradient-based
		Stochastic or deterministic start points, or combination of both
		Automatic stochastic start points
		Runs all start points
Patternsearch	Proven convergence to local optimum; slower than gradient-based solvers	Deterministic iterates
		Can run in parallel
		No gradients
		User-supplied start point
Surrogate Optimization	Proven convergence to global optimum for bounded problems; slower than gradient-based solvers; generally stops by reaching a function evaluation limit	Stochastic iterates
		Can run in parallel
		Best use for time-consuming objective functions
		Requires bound constraints, accept linear constraints and nonlinear inequality constraints
		Allows integer constraints
		No gradients
		Automatic start points or user-supplied points, or combination of both
Particleswarm	No convergence proof	Stochastic iterates
		Can run in parallel
		Population-based
		No gradients
		Automatic start population or user-supplied population, or combination of both
		Only bound constraints
Genetic Algorithm	No convergence proof	Stochastic iterates
		Can run in parallel
		Population-based
		No gradients
		Allows integer constraints
		Automatic start population or user-supplied population, or combination of both
Simulated Annealing	Proven to converge to global optimum for bounded problems withvery slow cooling schedule	Stochastic iterates
		No gradients
		User-supplied start point
		Only bound constraints

the dimension of the decision variables. Genetic algorithm and surrogate optimization do not require any starting points because they take the dimension of the decision variables as an input or infer dimensions from bounds. These solvers automatically generate a start point or population, or they accept a point or point that is supplied [82].

Surrogate optimization is used for problems that have time-consuming objective functions. It searches for a global solution, requires finite bounds, and accepts an integer, linear, and nonlinear inequality constraints. The problem is large-scale, nonlinear, and binary integer programming. Although genetic algorithm fail to converge for some problems, they are proven to be often effective and can handle all types of constraints. Genetic algorithm and surrogate optimization are the only global optimization toolbox solvers that accept integer constraints. Therefore, genetic algorithm and surrogate optimization are selected for the optimization process for optimal blocking device placement in the thesis. The simulation results of the total number of BDs and candidate transformers for BD placement in their neutrals obtained from both methods are presented in chapter 5.

Genetic algorithm solves smooth or non-smooth optimization problems with any type of constraint, including integer constraints. It is a stochastic, population-based algorithm that searches randomly by mutation and crossover among population members. The genetic algorithm begins by creating a random initial population. The algorithm then creates a sequence of new populations. At each step, the algorithm uses the individuals in the current generation to create the next population. To create the new population, the algorithm performs the following steps: 1) Scores each member of the current population by computing its fitness value. These values are called the raw fitness scores. 2) Scales the raw fitness scores to convert them into a more usable range of values. These scaled values are called expectation values. 3) Selects members, called parents, based on their expectation. 4) Some of the individuals in the current population that have lower fitness are chosen as elite. These elite individuals are passed on to the next population. 5) Produces children from the parents. Children are produced either by making random changes to a single parent—mutation—or by combining the vector entries of a pair of parents—crossover. 6) Replaces the current

population with the children to form the next generation. The algorithm stops when one of the stopping criteria is met.

A surrogate is a function that approximates another function. The surrogate is useful because it takes little time to evaluate. To search for a point that minimizes an objective function, it simply evaluates its surrogate on thousands of points and takes the best value as an approximation to the minimizer of the objective function. Surrogate optimization attempts to find a global minimum of an objective function using a few objective function evaluations. To do so, the algorithm tries to balance the optimization process between two goals: exploration and speed, exploration to search for a global minimum, and speed to obtain a good solution in a few objective function evaluations. The algorithm has been proven to converge to a global solution for continuous objective functions on bounded domains [83]. The surrogate optimization algorithm alternates between two phases: 1) construct surrogate — create random points within the bounds, evaluate the (expensive) objective function at these points and construct a surrogate of the objective function by interpolating a radial basis function through these points and 2) search for minimum — search for a minimum of the objective function by sampling several thousand random points within the bounds, evaluate a merit function based on the surrogate value at these points and on the distances between them and points where the (expensive) objective function has been evaluated, choose the best point as a candidate, as measured by the merit function, evaluate the objective function at the best candidate point, the point is called an adaptive point, update the surrogate using this value and search again. The algorithm stops the search for the minimum phase when all the search points are too close to points where the objective function was previously evaluated [82].

Chapter 5

Simulation Results and Discussion

As mentioned in the above chapters, BD placement optimization is done in the IEEE 118-bus standard test system. For the simulation, the geoelectric field derived from the 1989 Hydro Quebec event is used and scaled from $E = 1\,V/km$ to $8\,V/km$ to describe scenarios at different levels of geoelectric field E. The data from the event was recorded for 1440 minutes. Therefore, all the data and results are based on the data from that time frame. The effects of a geomagnetic disturbance event and its associated geoelectric field on the voltage magnitude of system buses and the hotspot temperature of transformers are studied and presented in the following sections. The results of the proposed optimal BD placement approach are also presented, where both bus voltages and hotspot temperature of transformers are maintained within limits.

5.1 Impacts of GIC on System Voltages

This section illustrates the negative impacts of GMD events on the power system voltages. The system voltages are calculated for different values of the geoelectric field ($E = 1\,V/km$ to $E = 8\,V/km$). The results of the calculation are demonstrated in the Figure 5.1 to Figure 5.8 that indicate the GMD causes the voltage drop in some of the system buses to the extent where it drops below the minimum permissible voltage 0.94 $p.u.$ and with the increase in the intensity of GMD, the voltage drop is more pronounced. To illustrate this, the voltage at buses 115 and 53 is depicted at different levels of E. Bus 115 and 53 were taken into reference because they have the minimum voltage among all the buses and are not in close proximity to each other.

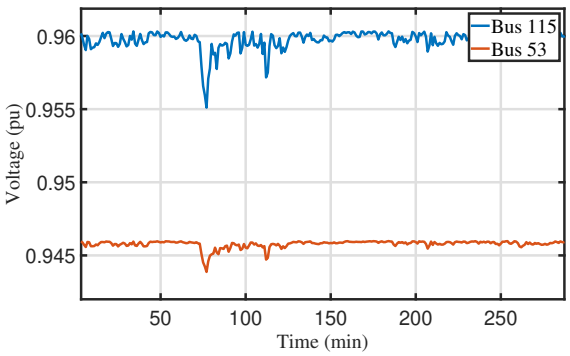

Figure 5.1: Voltage ($p.u.$) at bus 115 and 53 at $E = 1\,V/km$ (without BD).

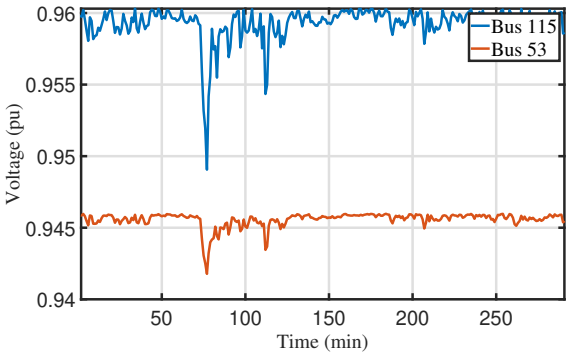

Figure 5.2: Voltage ($p.u.$) at bus 115 and 53 at $E = 2\,V/km$ (without BD).

Figure 5.1 to Figure 5.8 show the voltages at bus 115 and 53 at different levels of E ($E = 1\,V/km$ to $E = 8\,V/km$) respectively without BD placement. The figures are zoomed in to show the transitions more clearly. It is seen from Figure 5.1 and Figure 5.2 that the minimum voltage at $E = 1\,V/km$ and $E = 2\,V/km$ does not drop below minimum permissible

voltage 0.94 $p.u.$ whereas it can be less than the minimum permissible voltage at times for $E = 3\,V/km$ to $E = 8\,V/km$ as seen in Figure 5.3 to Figure 5.8. The minimum voltage is at bus 115 and is 0.9196 $p.u.$ at $E = 3\,V/km$, 0.8879 $p.u.$ at $E = 4\,V/km$, 0.8586 $p.u.$ at $E = 5\,V/km$, 0.8297 $p.u.$ at $E = 6\,V/km$, 0.8010 $p.u.$ at $E = 7\,V/km$ and 0.7736 $p.u.$ at $E = 8\,V/km$. So, from the figures, it can be seen that the voltage drop is more pronounced as the intensity of GMD increases.

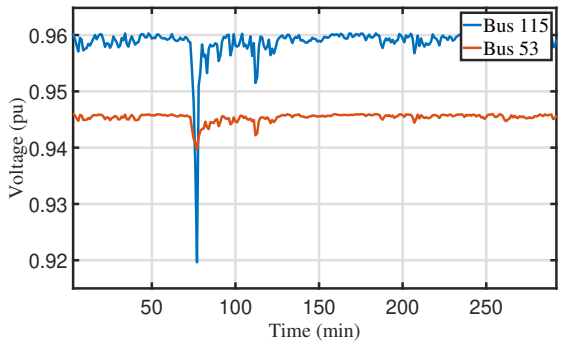

Figure 5.3: Voltage ($p.u.$) at bus 115 and 53 at $E = 3\,V/km$ (without BD).

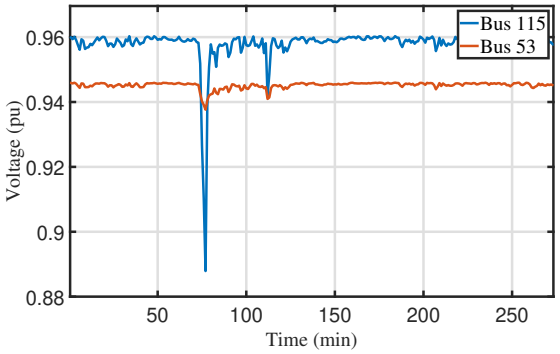

Figure 5.4: Voltage ($p.u.$) at bus 115 and 53 at $E = 4\,V/km$ (without BD).

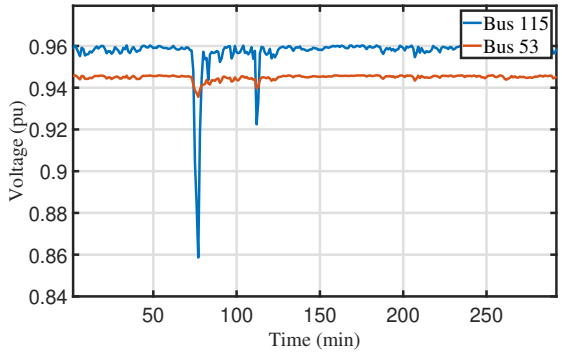

Figure 5.5: Voltage ($p.u.$) at bus 115 and 53 at $E = 5\,V/km$ (without BD).

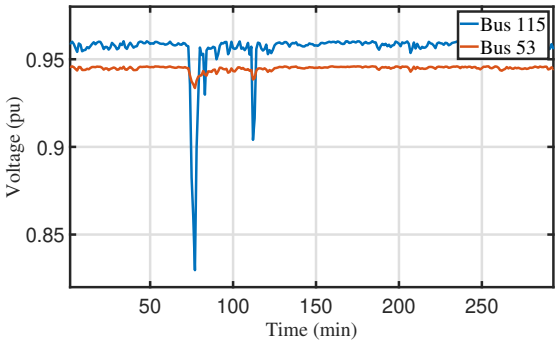

Figure 5.6: Voltage ($p.u.$) at bus 115 and 53 at $E = 6\,V/km$ (without BD).

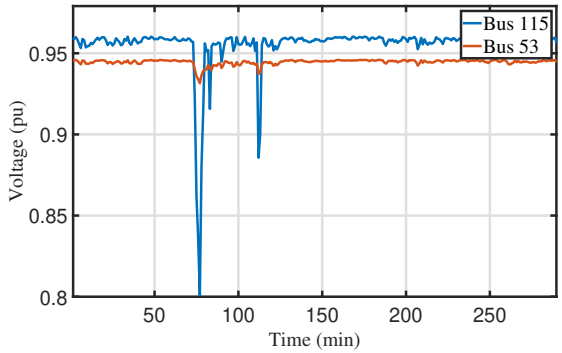

Figure 5.7: Voltage ($p.u.$) at bus 115 and 53 at $E = 7\,V/km$ (without BD).

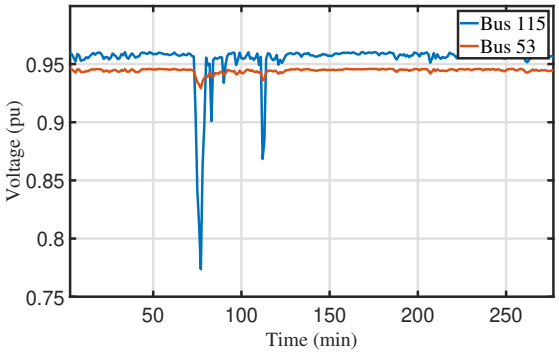

Figure 5.8: Voltage ($p.u.$) at bus 115 and 53 at $E = 8\,V/km$ (without BD).

5.2 Impacts of GIC on Transformer Hotspot Temperature

This section demonstrates the negative impacts of GIC on transformer hotspot temperature at its winding and other structural parts, such as tie-plates. The hotspot temperature rise of transformer winding and tie-plate is calculated for different levels of geoelectric field ($E = 1\,V/km$ to $E = 8\,V/km$) and are presented. The calculation results indicate that the GMD causes hotspot temperature rise of transformers' windings and tie-plates above the maximum temperature limit. With the increase in the intensity of GMD, the hotspot temperature rise is more prominent and higher, which could cause damage to transformers.

Table 5.1 to 5.6 shows the transformers with their respective tie-plate and winding temperatures that are greater than the maximum temperature limit of $200\,^{\circ}C$ for tie-plate and $180\,^{\circ}C$ for winding at different levels of E ($E = 3\,V/km$ to $E = 8\,V/km$). No transformer has its hotspot temperature rise more than the maximum limit at $E = 1\,V/km$ and $E = 2\,V/km$. It is seen that the transformer winding temperature does not cross the maximum limit of

180 $°C$ at $E = 3\,V/km$, $E = 4\,V/km$ and $E = 5\,V/km$. Only two transformers have winding temperature more than 180 $°C$ at $E = 6\,V/km$, seven transformers have winding temperature more than 180 $°C$ at $E = 7\,V/km$ and nine transformers have winding temperature more than 180 $°C$ at $E = 8\,V/km$. It is seen from the tables below that those transformers with their winding temperature more than the maximum limit of 180 $°C$ have their tie-plate temperature more than approximately 400 $°C$.

Table 5.1: Most critical transformers and associated hotspot temperatures for $E = 3\,V/km$ before BD placement

Transformer Number	Maximum Tie-plate Temperature ($°C$)	Maximum Winding Temperature ($°C$)
19	265.8	143.5
22	237.2	135.8
24	243.8	137.5
40	221.5	131.8
84	265.8	143.5
85	237.2	135.8
89	243.8	137.5
119	221.5	131.8
159	240.5	136.7

The transformers in the tables are separated on the basis if they are required to be repaired or replaced based on their hotspot temperature. The transformers with their hotspot temperature more than 1.5 times the maximum temperature limit are considered to be replaced, and those transformers with their hotspot temperature more than the maximum temperature limit but less than 1.5 times the maximum temperature limit are considered to be repaired. Since the transformers with their winding temperature over the maximum temperature limit of 180 $°C$ have their tie-plate temperature more than 400 $°C$, those transformers are all

Table 5.2: Most critical transformers and associated hotspot temperatures for $E = 4\,V/$ km before BD placement

Transformer Number	Maximum Tie-plate Temperature ($°C$)	Maximum Winding Temperature ($°C$)
14	205.5	128.3
19	320.2	157.7
22	281.6	147.4
24	290.6	149.7
27	220.2	131.0
40	260.3	142.1
45	200.1	126.0
83	228.3	133.4
84	320.2	157.7
85	281.6	147.4
89	290.6	149.7
94	205.1	127.1
95	220.2	131.0
119	260.3	142.1
125	200.1	126.0
158	211.1	128.9
159	286.2	148.6

considered to be replaced. Therefore, all the transformers with winding temperatures more than $180\,°C$ and the transformers whose tie-plate temperature is more than 1.5 times of maximum temperature limit are considered to be replaced. No transformer needs to be replaced at $E = 1\,V/km$ to $E = 3\,V/km$ and all the transformers mentioned in Table 5.1 are considered to be repaired. The shaded transformers in Table 5.2 to 5.6 present the transformers that are considered to be replaced with their respective tie-plate and winding temperatures at $E = 4\,V/km$ to $E = 8\,V/km$ while the rest of the transformers in the tables are considered to be repaired.

Table 5.3: Most critical transformers and associated hotspot temperatures for $E = 5\,V/$ km before BD placement

Transformer Number	Maximum Tie-plate Temperature	Maximum Winding Temperature
14	229.7	134.9
19	374.6	171.9
22	326.4	159.1
24	337.5	161.9
27	248.2	138.5
40	299.7	152.4
45	223.7	132.3
83	259.1	141.6
84	374.6	171.9
85	326.4	159.1
89	337.5	161.9
94	229.4	133.6
95	248.2	138.5
96	204.2	126.9
119	299.7	152.4
125	223.7	132.3
158	237.7	135.9
159	332.0	160.5

Table 5.4: Most critical transformers and associated hotspot temperatures for $E = 6\,V/$ km before BD placement

Transformer Number	Maximum Tie-plate Temperature ($^{\circ}C$)	Maximum Winding Temperature ($^{\circ}C$)
6	200.7	125.8
9	216.4	128.8
14	257.4	141.6
19	428.9	186.0
22	371.1	170.7
24	384.4	174.0
27	277.4	146.0
31	203.0	127.1
40	339.1	162.7
45	247.4	138.5
83	290.4	149.7
84	428.9	186.0
85	371.1	170.7
89	384.4	174.0
94	254.1	140.1
95	277.4	146.0
96	223.4	132.1
109	203.0	127.1
119	339.1	162.7
125	247.4	138.5
158	264.3	142.9
159	377.8	172.4

Table 5.5: Most critical transformers and associated hotspot temperatures for $E = 7\,V/$ km before BD placement

Transformer Number	Maximum Tie-plate Temperature	Maximum Winding Temperature
6	216.0	130.0
9	234.5	133.5
14	282.8	148.2
19	483.2	200.1
22	415.8	182.3
23	207.1	127.9
24	431.3	186.2
27	306.5	153.6
31	218.8	131.2
40	378.5	173.0
45	271.4	144.8
56	212.0	129.3
83	321.7	157.9
84	483.2	200.1
85	415.8	182.3
86	210.2	128.7
88	207.1	127.9
89	431.3	186.2
94	279.4	146.7
95	306.5	153.6
96	243.1	137.3
109	218.8	131.2
119	378.5	173.0
125	271.4	144.8
126	206.4	127.5
149	212.0	129.3
158	291.2	149.9
159	423.6	184.3

Table 5.6: Most critical transformers and associated hotspot temperatures for $E = 8\,V/$ km before BD placement

Transformer Number	Maximum Tie-plate Temperature ($°C$)	Maximum Winding Temperature ($°C$)
6	231.6	134.2
9	253.3	138.2
14	308.3	154.8
18	211.8	129.1
19	537.5	214.3
22	460.4	193.8
23	221.8	131.7
24	478.2	198.3
27	335.5	161.1
31	235.1	135.2
40	417.5	183.2
45	295.5	151.1
56	227.4	133.3
62	211.1	128.5
76	210.3	128.4
79	211.8	129.1
83	352.9	166.0
84	537.5	214.3
85	460.4	193.9
86	225.4	132.8
88	221.8	131.7
89	478.2	198.3
94	304.7	153.2
95	335.5	161.1
96	262.9	142.5
109	235.1	135.2
119	417.9	183.2
125	295.5	151.1
126	220.4	131.3
149	227.4	133.3
157	211.1	128.5
158	318.2	156.8
159	469.4	196.1

To illustrate this, the temperature rise at both tie-plate and winding of transformer number 19 superimposed on the computed GIC current is shown in the figures below for different levels of geoelectric field ($E = 1\,V/km$ to $E = 8\,V/km$). Transformer number 19 is selected to illustrate the result because transformer 19 and 84 are the most affected and vulnerable transformers, with hotspot temperature rise in these transformers more prominent than the others. Since they both have a similar temperature rise, that of 19 is presented.

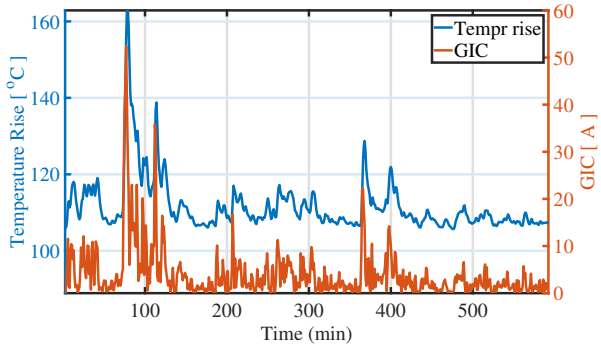

Figure 5.9: Temperature rise ($°C$) at transformer 19 tie-plate at $E = 1\,V/km$ (without BD).

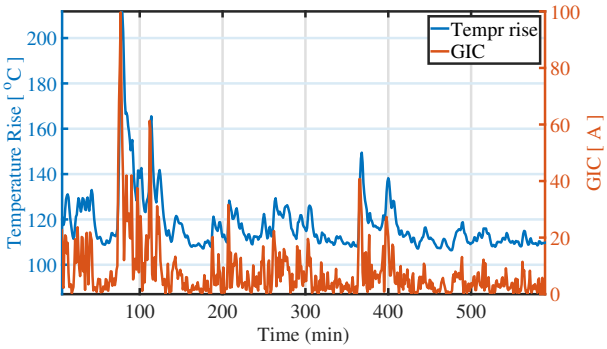

Figure 5.10: Temperature rise ($°C$) at transformer 19 tie-plate at $E = 2\,V/km$ (without BD).

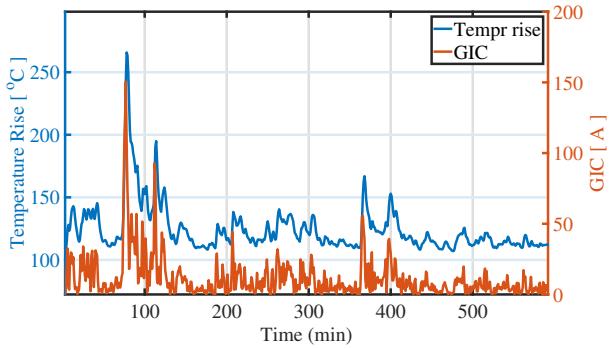

Figure 5.11: Temperature rise ($°C$) at transformer 19 tie-plate at $E = 3\,V/km$ (without BD).

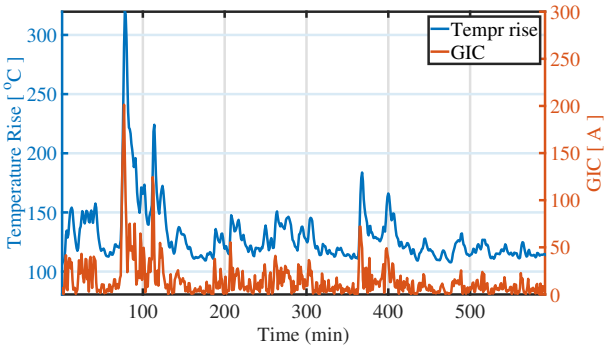

Figure 5.12: Temperature rise ($°C$) at transformer 19 tie-plate at $E = 4\,V/km$ (without BD).

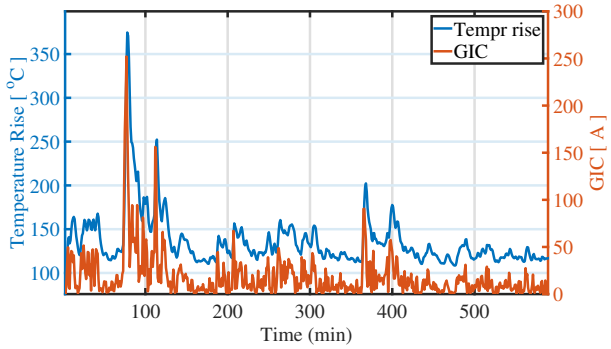

Figure 5.13: Temperature rise ($°C$) at transformer 19 tie-plate at $E = 5\,V/km$ (without BD).

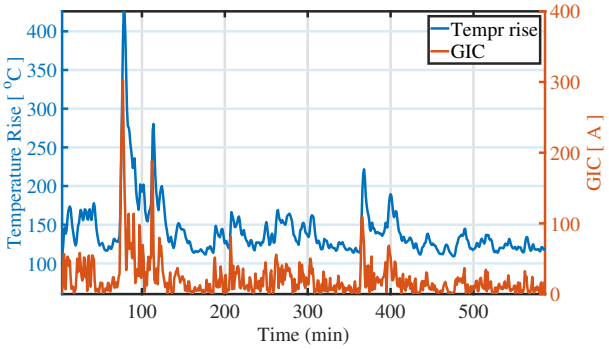

Figure 5.14: Temperature rise ($°C$) at transformer 19 tie-plate at $E = 6\,V/km$ (without BD).

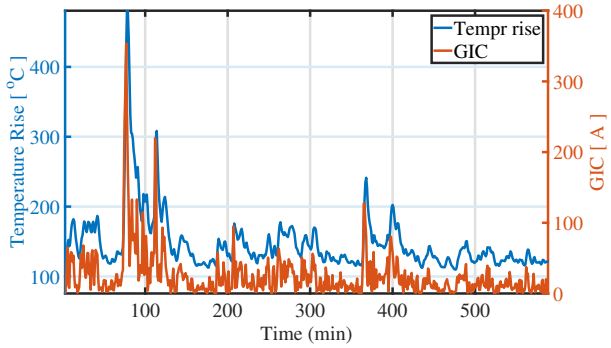

Figure 5.15: Temperature rise ($°C$) at transformer 19 tie-plate at $E = 7\,V/km$ (without BD).

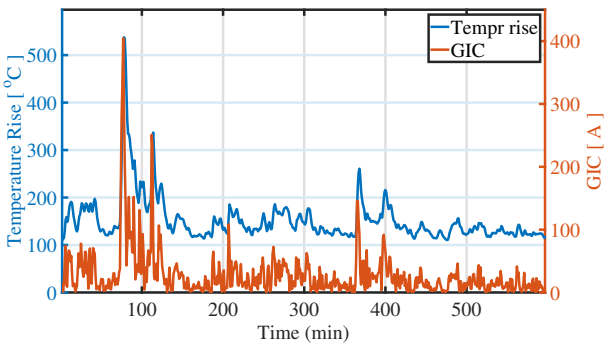

Figure 5.16: Temperature rise ($°C$) at transformer 19 tie-plate at $E = 8\,V/km$ (without BD).

Figure 5.9 to Figure 5.16 show the absolute value of the computed GIC current, superimposed on the tie-plate temperature rise in Transformer 19 for different levels of E ($E = 1\,V/km$ to $E = 8\,V/km$). It is seen from Figure 5.9 that the hotspot temperature rise of the tie-plate of transformer 19 does not cross the maximum limit of $200\,°C$ but in Figure 5.10 to Figure. 5.16, the maximum temperature rise of tie-plate of that transformer is more than the maximum limit of $200\,°C$ for $E = 2\,V/km$ to $E = 8\,V/km$. Similarly, Figure 5.17

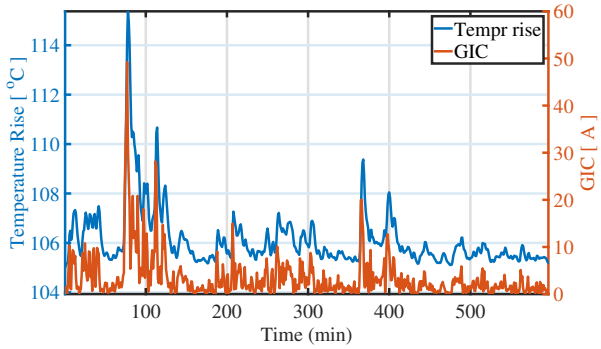

Figure 5.17: Temperature rise ($°C$) at transformer 19 winding at $E = 1\,V/km$ (without BD).

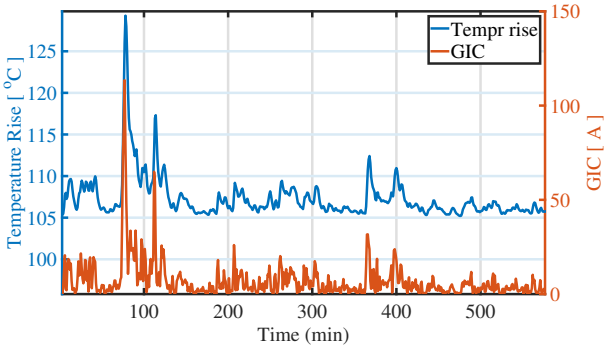

Figure 5.18: Temperature rise ($°C$) at transformer 19 winding at $E = 2\,V/km$ (without BD).

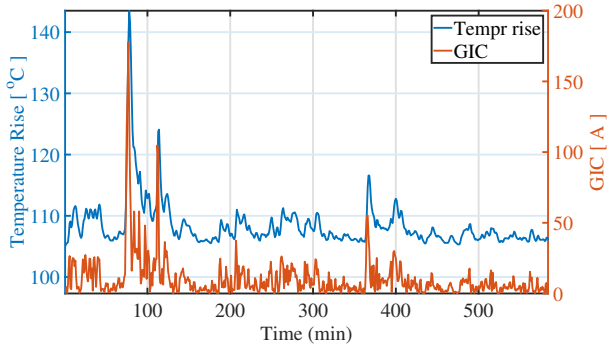

Figure 5.19: Temperature rise ($°C$) at transformer 19 winding at $E = 3\,V/km$ (without BD).

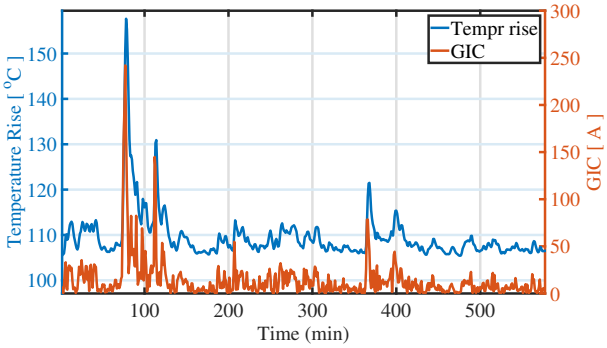

Figure 5.20: Temperature rise ($°C$) at transformer 19 winding at $E = 4\,V/km$ (without BD).

to Figure 5.24 show the absolute value of the computed GIC, superimposed on the hotspot temperature rise in the winding of transformer 19 for different levels of E ($E = 1\,V/km$ to $E = 8\,V/km$). For the temperature rise of winding of the transformer, it is seen from Figure 5.17 to Figure 5.21 that the maximum temperature rise of the winding of transformer is below the maximum temperature limit of $180\,°C$ for values of E from $1\,V/km$ to $E = 5\,V/km$ while the temperature rise is more than the maximum limit for $E = 6\,V/km$ to $E = 8\,V/km$ as

seen in Figure 5.22 to Figure 5.24. The figures show that the maximum temperature rise in the transformer hotspot is significantly higher for both tie-plate and winding as the intensity of GMD increases and as the magnitude of GIC increases. We can see that the maximum temperature rise is more than 500 $°C$ at the tie-plate and is more than 200 $°C$ at the winding of the transformer at $E = 8\,V/km$ which is a severe temperature rise.

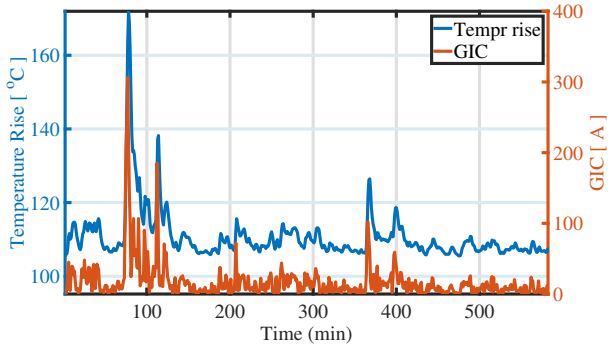

Figure 5.21: Temperature rise ($°C$) at transformer 19 winding at $E = 5\,V/km$ (without BD).

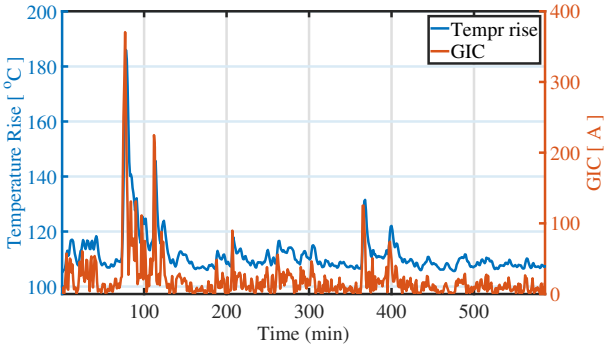

Figure 5.22: Temperature rise ($°C$) at transformer 19 winding at $E = 6\,V/km$ (without BD).

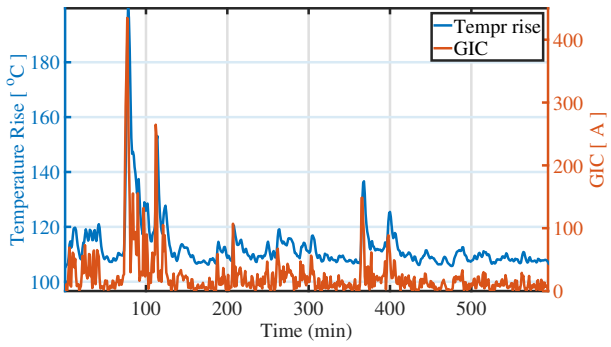

Figure 5.23: Temperature rise ($°C$) at transformer 19 winding at $E = 7\,V/km$ (without BD).

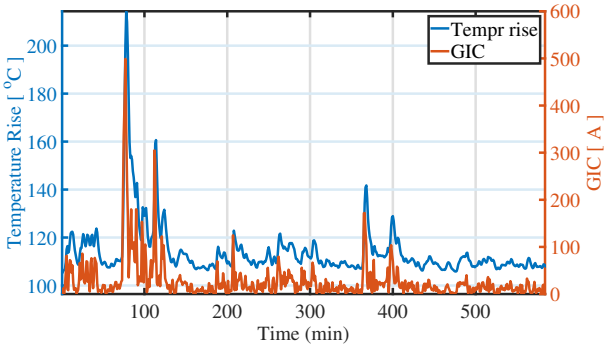

Figure 5.24: Temperature rise ($°C$) at transformer 19 winding at $E = 8\,V/km$ (without BD).

5.3 Optimal Placement of Blocking Device

In the thesis, two methods of optimization from MATLAB optimization toolbox [82], Surrogate Optimization [84], and Genetic Algorithm [85, 86] are used to find the optimal number of blocking devices (BDs) and their placement on specific transformers. The problem is large-scale, nonlinear, binary integer programming and requires an excessive computation time to evaluate all 2^{162} possible combinations. Surrogate Optimization (SO) and Genetic Algorithm (GA) from the MATLAB optimization toolbox are selected as discussed in chapter 4. Surrogate optimization is used for expensive optimization functions and is comparatively easier. GA is stochastic in nature and the results obtained in every simulation are different, so the best-obtained results are presented. The problem is solved for different levels of E ($E = 1\,V/km$ to $8\,V/km$) with a total number of candidate transformers being 162. First, it is done in surrogate optimization for $E = 1\,V/km$ to $E = 8\,V/km$, and then it is done with genetic algorithm and compared to the results of surrogate optimization. The results from both methods SO and GA are presented in the sections below.

5.3.1 Surrogate Optimization

The optimization algorithm, as mentioned before in the chapter 4 is that the most critical transformers are identified for each levels of E and the blocking devices are placed on the neutral of these transformers and the number of BDs is optimized. The initial population $x_i = 0$ for $i = 1, 2, \ldots, n$, n being the total number of candidate transformers, is used for lower values of E but as we go for higher E, the problem becomes very time-consuming and the solution does not converge to the optimal value as it converges to the local minimum

rather than global minimum. So, for higher values of E, first, the most critical transformers are identified based on their hotspot temperature rise, i.e., whose maximum temperature rise is more than the maximum temperature limit for each E. These transformers are taken as the initial population for the optimization process, and the optimized number of BDs is identified, and the candidate transformers for BD placement are identified.

Table 5.7: Optimal number of BDs for various GMD intensities using surrogate optimization

$E\ (V/km)$	$2\,V/km$	$3\,V/km$	$4\,V/km$	$5\,V/km$	$6\,V/km$	$7\,V/km$	$8\,V/km$
BD	2	6	13	15	19	24	28

Table 5.8: Candidate transformers for BD placement for $E = 2\,V/km$ to $8\,V/km$ after optimization (surrogate optimization)

E (V/km)	Candidate Transformers for GIC Blocking Device Placement (Surrogate Optimization)
2	19 84
3	19 24 84 89 158 159
4	14 19 24 44 56 83 84 89 94 124 149 158 159
5	14 19 22 24 27 40 45 83 84 89 95 119 125 158 159
6	6 9 14 19 24 27 31 40 45 83 84 89 95 109 119 125 128 158 159
7	6 9 14 19 22 24 27 31 40 45 46 56 83 84 85 89 95 109 119 125 128 149 158 159
8	6 9 14 18 19 22 24 27 31 40 45 46 56 76 79 83 84 85 86 89 95 109 119 125 128 149 158 159

Table 5.7 shows the result of the optimization process given the total number of BDs for each level of E ($E = 2\,V/km$ to $E = 8\,V/km$) using surrogate optimization from Matlab optimization toolbox. Table 5.8 shows the candidate transformers for the BD placement for each level of E ($E = 2\,V/km$ to $8\,V/km$). At $E = 1\,V/km$, there is no voltage violation, and none of the transformers' tie-plate and winding temperatures are beyond the maximum

limit, so no BD is required. There is no voltage violation in the case of $E = 2\,V/km$, but two transformers' tie-plate temperatures are more than $200\,°C$, transformer number 19 and 84. Thus, BD should be placed at these two transformers to limit the two transformers' tie-plate temperature below $200\,°C$. For $E = 3\,V/km$ to $E = 8\,V/km$, there is voltage violation and temperature rise beyond the maximum limit, so BDs should be placed to maintain bus voltage and transformer temperature rise. As a result, the total number of BDs and the candidate transformers are identified using the optimization process. Although the winding temperatures of transformers are within the maximum limit of $180\,°C$ until $E = 5\,V/km$, BDs are required to limit the temperatures of the tie-plate of transformers below $200\,°C$. Table 5.8 shows that the number of candidate transformers after optimization is lower than the number of transformers with temperatures higher than the limit as presented in above Table 5.1 to Table 5.6 and are not necessarily the same transformers. For higher GMD, the candidate transformers are similar.

As we go for higher E, say $E = 6\,V/km$ to $8\,V/km$, there are two auto-transformers whose tie-plate temperature is more than $200\,°C$ as seen in Table. 5.4 to 5.6. For $E = 6\,V/km$, the maximum temperature of the tie-plate is just above $200\,°C$; therefore, only the neutral blockers are enough to maintain the temperature below the maximum limit. But for $E = 7\,V/km$ and $E = 8\,V/km$, even if we place neutral blocker in the neutral connected to the common winding of these transformers, the GIC flows through the LV side; therefore, it does not completely block GIC and temperature is still high. So, to limit temperature rise in this type of transformer, only neutral blocker is not enough and series capacitor blocker is required to be placed. But series capacitor blockers are primarily used for series compensation of transmission lines but have a secondary effect of blocking dc current flow in transmission lines and are more costly. Even after running the optimization problem a number of times, the

temperature rise at transformer number 9 would not come within the maximum limit even with a large number of neutral blockers. Therefore, series capacitor blocker is required and is placed at line 115 for $E = 7\,V/km$ and at 115 and 116 for $8\,V/km$. Line 115 is obtained such that transformer number 9 is connected to buses 80 and 81, so the lines connected to buses 80 and 81 were 115, 116, 117, and 118. Since we are trying to make the cost as minimum as possible, it is not required to place series capacitor blocker at all these mentioned lines because placing it in one or two lines would be enough to maintain the temperature rise. For $E = 7\,V/km$, the series capacitor blocking at line 115 was enough, so further optimization was done with only one series capacitor blocking. While for $8\,V/km$, series capacitor blockers at lines 115 and 116 were required, and then further optimization was done. This applies to both of the optimization solvers.

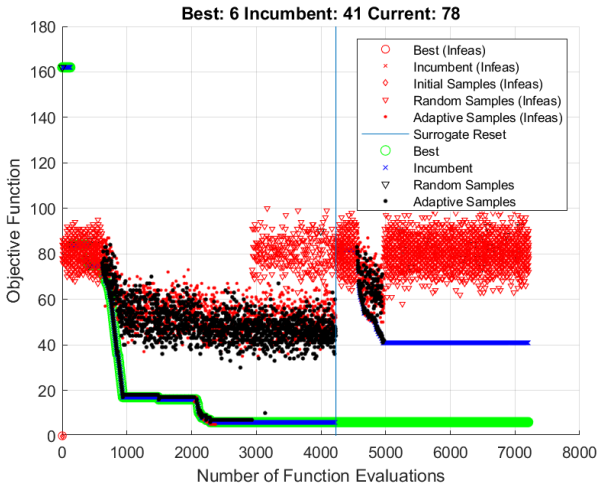

Figure 5.25: Best value at $E = 3\,V/km$ (surrogate optimization).

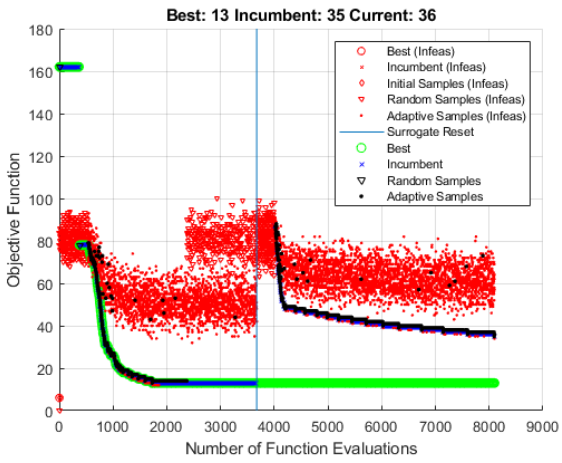

Figure 5.26: Best value at $E = 4\,V/km$ (surrogate optimization).

Figure 5.25 to Figure 5.30 illustrates the results of optimization process and shows the best value of the optimization function by using surrogate optimization from the MATLAB

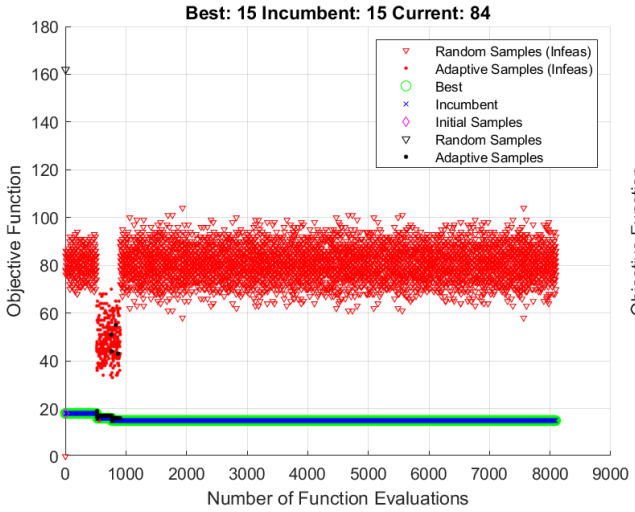

Figure 5.27: Best value at $E = 5\ V/km$ (surrogate optimization).

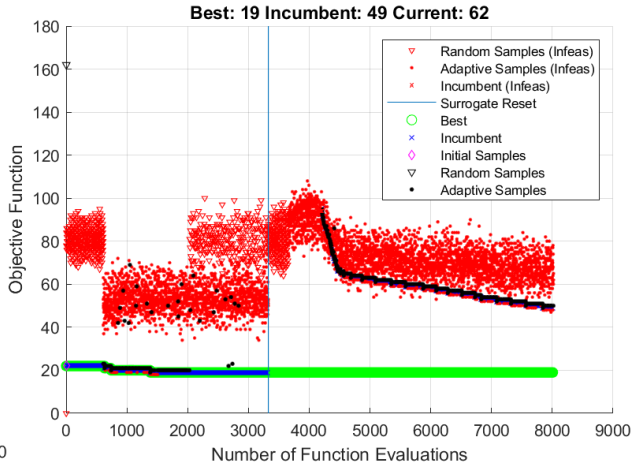

Figure 5.28: Best value at $E = 6\ V/km$ (surrogate optimization).

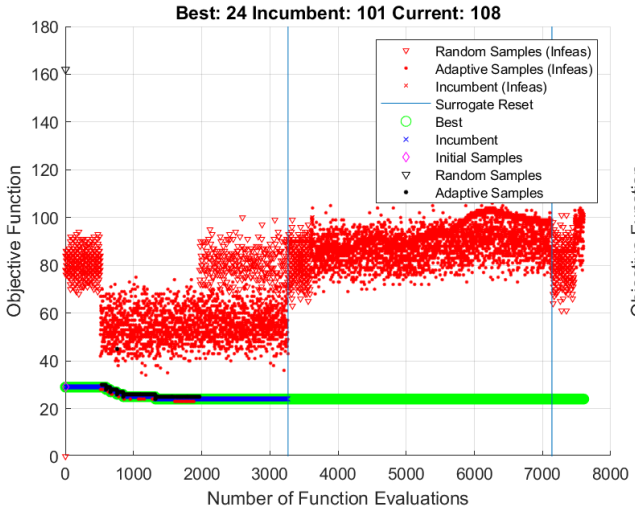

Figure 5.29: Best value at $E = 7\ V/km$ (surrogate optimization).

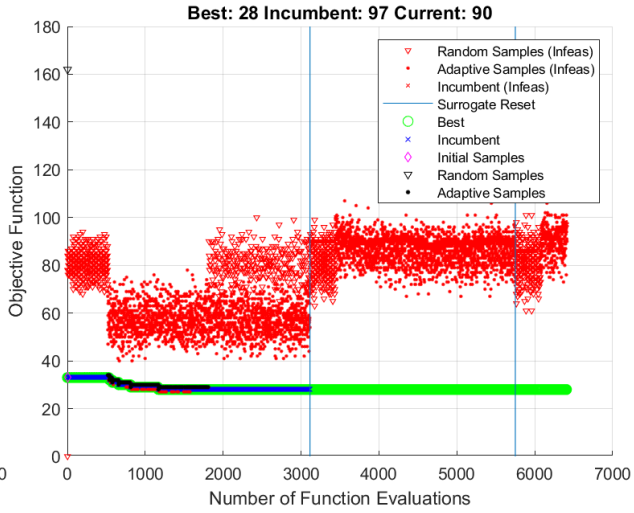

Figure 5.30: Best value at $E = 8\ V/km$ (surrogate optimization).

optimization toolbox for each level of E ($E = 3\ V/km$ to $E = 8\ V/km$). As shown in the figures, the best value is basically the point with the smallest objective function value among

all evaluated so far, which is the optimized number of BDs required to block the GIC so that none of the constraints is violated.

5.3.1.1 Results after BD placement (surrogate optimization)

Figure 5.31 to Figure 5.37 show the voltage at bus 115 and 53 after BD placement at different level of E ($E = 2\,V/km$ to $8\,V/km$) using surrogate optimization. The voltage drop was more pronounced at buses 115 and 53, so the voltage improvement at these buses after placing BDs is presented. At $E = 2\,V/km$, the minimum voltage at bus 115 was improved to $0.9491\,p.u.$ and voltage at bus 53 was improved to $0.9418\,p.u.$ as seen in Figure 5.31 after BD placement at transformers 19 and 84 as mentioned in Table 5.8. At $E = 3\,V/km$, the minimum voltage of bus 115 is increased above $0.94\,p.u.$ and is $0.96\,p.u.$ and bus 53 voltage reaches the minimum of $0.9397\,p.u.$, after placing BDs as presented in Table 5.8. To further increase it above $0.94\,p.u.$, the load is decreased to 95% as it is more cost-effective than placing another BD. It is seen that the voltage is improved to $0.9404\,p.u.$ and is in the acceptable range as seen in Figure 5.32.

At $E = 4V/km$, the minimum voltage at bus 115 is more than $0.96\,p.u.$, but the minimum voltage at bus 53 was $0.9376\,p.u.$ after placing BDs as mentioned in the above table. So, the total load is decreased to 80% to maintain the bus voltage of bus 53 above $0.94\,p.u.$ and is improved to $0.9402\,p.u.$ as seen in Figure 5.33. Similarly, for $E = 5V/km$, the minimum voltage at bus 115 is more than $0.96\,p.u.$, and the minimum voltage at bus 53 was $0.9356\,p.u.$ after placing BDs. So, the total load is decreased to 60% to maintain bus voltage at bus 53 above $0.94\,p.u.$ and is improved to $0.9405\,p.u.$ as seen in Figure 5.34. Furthermore, placing BDs at the transformer neutrals mentioned on Table 5.8 makes that the voltage improvement

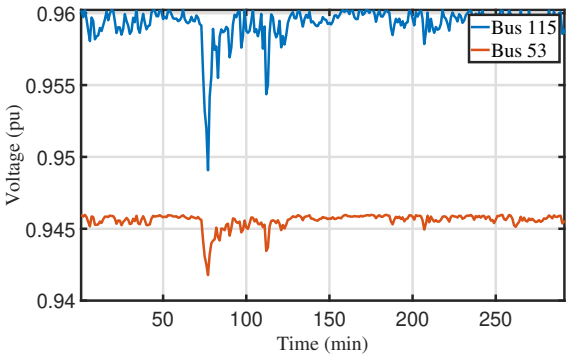

Figure 5.31: Voltage ($p.u.$) at bus 115 and 53 at $E = 2\,V/km$ (with BD, surrogate optimization).

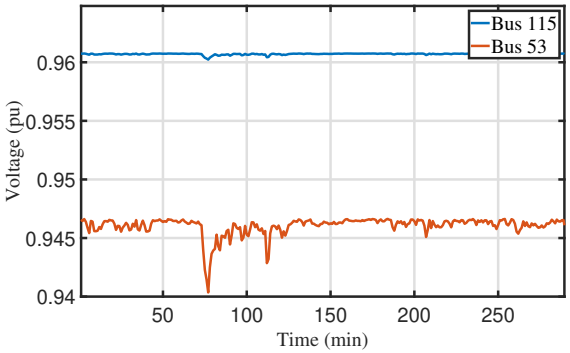

Figure 5.32: Voltage ($p.u.$) at bus 115 and 53 at $E = 3\,V/km$ (with BD, surrogate optimization).

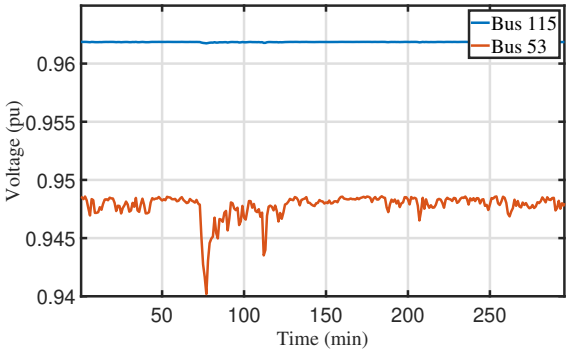

Figure 5.33: Voltage ($p.u.$) at bus 115 and 53 at $E = 4\,V/km$ (with BD, surrogate optimization).

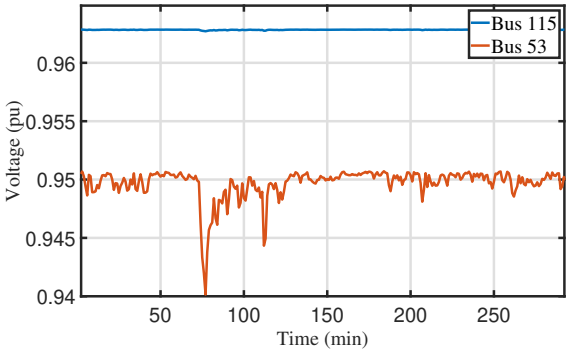

Figure 5.34: Voltage ($p.u.$) at bus 115 and 53 at $E = 5\,V/km$ (with BD, surrogate optimization).

at $E = 6\,V/km$ above $0.94\,p.u.$ for all buses but $0.9329\,p.u.$ at bus 53. Decreasing load does not improve the voltage profile, so placing another BD at the transformer connected to bus 53, i.e., transformer number 108, is the only solution. Figure 5.35 shows the voltage improvement above $0.94\,p.u.$ after placing an additional BD at transformer number 108's neutral. Similarly, BD in transformer number 108 is required to maintain bus voltages greater than $0.94\,p.u.$

at all buses for $E = 7\,V/km$ and $E = 8\,V/km$ and the voltage improvement is as shown in Figure 5.36 and Figure 5.37.

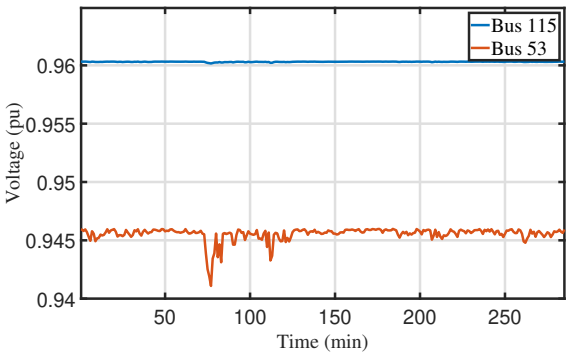

Figure 5.35: Voltage ($p.u.$) at bus 115 and 53 at $E = 6\,V/km$ (with BD, surrogate optimization).

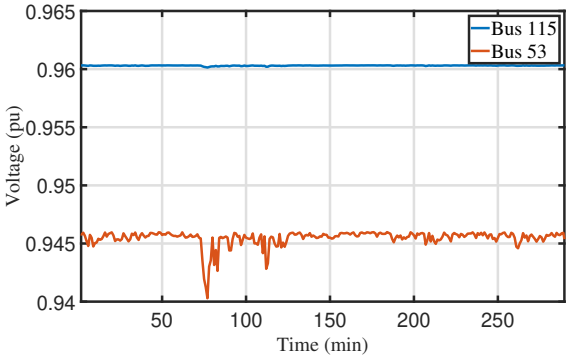

Figure 5.36: Voltage ($p.u.$) at bus 115 and 53 at $E = 7\,V/km$ (with BD, surrogate optimization).

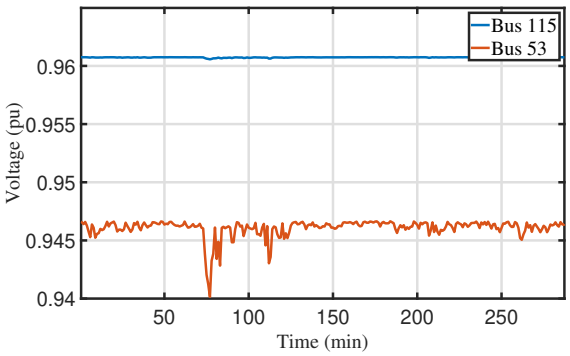

Figure 5.37: Voltage ($p.u.$) at bus 115 and 53 at $E = 8\,V/km$ (with BD, surrogate optimization).

The hotspot temperature rise of the transformer number 19 after BD placement is decreased to much extent, and is shown in Figure 5.38 to Figure 5.43 for both tie-plate and winding of the transformer at $E = 3\,V/km$, $6\,V/km$ and $8\,V/km$. The results of only

$E = 3\,V/km$, $6\,V/km$, and $8\,V/km$ are taken because the results for all E are similar as the GIC through the transformers is zero after placing BDs, and hence only temperature that is seen is the temperature of top oil of transformer which is $105\,°C$.

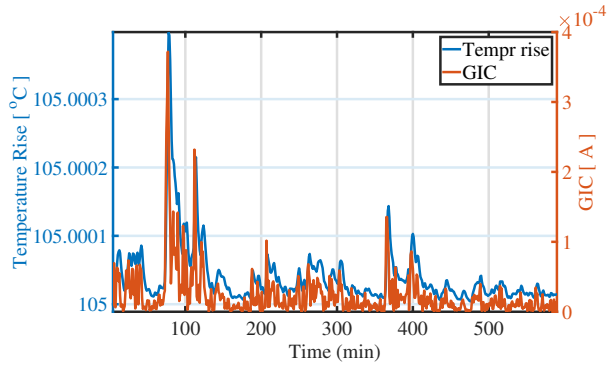

Figure 5.38: Temperature rise ($°C$) at transformer 19 tie-plate at $E = 3V/km$ (with BD, surrogate optimization).

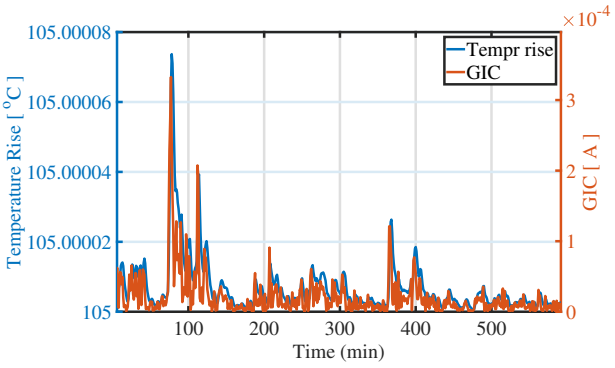

Figure 5.39: Temperature rise ($°C$) at transformer 19 tie-plate at $E = 3V/km$ (with BD, surrogate optimization).

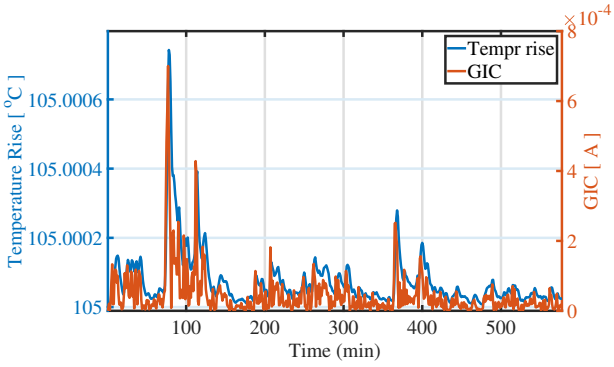

Figure 5.40: Temperature rise ($°C$) at transformer 19 tie-plate at $E = 6V/km$ (with BD, surrogate optimization).

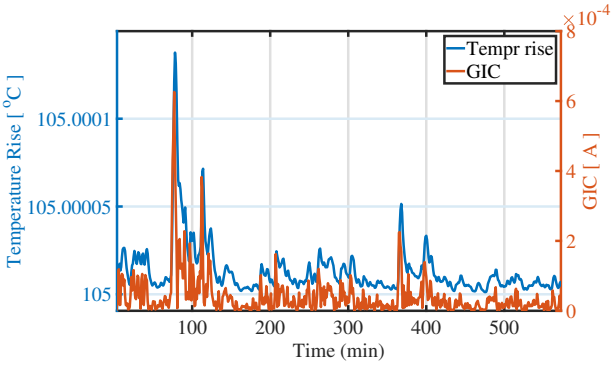

Figure 5.41: Temperature rise ($°C$) at transformer 19 tie-plate at $E = 6V/km$ (with BD, surrogate optimization).

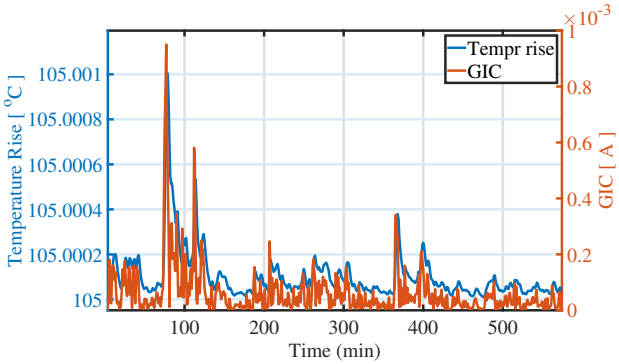

Figure 5.42: Temperature rise ($°C$) at transformer 19 tie-plate at $E = 8 V/km$ (with BD, surrogate optimization).

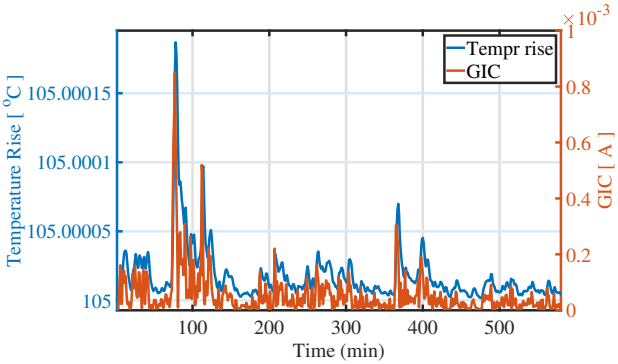

Figure 5.43: Temperature rise ($°C$) at transformer 19 tie-plate at $E = 8 V/km$ (with BD, surrogate optimization).

5.3.2 Genetic Algorithm

Table 5.9 shows the result of the optimization process given the total number of BDs for each levels of E ($E = 3\, V/km$ to $E = 8\, V/km$) using genetic algorithm from Matlab optimization toolbox. The initial population $x_i = 0$ for $i = 1, 2, \ldots, n$, n being the total number of candidate transformers. Table 5.10 presents the candidate transformers to which the BDs are placed on their neutrals. The main drawback of genetic algorithm is that it takes excessive time to compute and the best values of the objective function is different each time the program is simulated. So, the lowest values obtained from the genetic algorithm are presented here. The graphs showing the best value of the objective function for different level of E ($E = 3\, V/km$ to $E = 8\, V/km$) are shown in Figure 5.44 to Figure 5.49.

Table 5.9: Optimal number of BDs for various GMD intensities using genetic algorithm

$E\ (V/km)$	$3\ V/km$	$4\ V/km$	$5\ V/km$	$6\ V/km$	$7\ V/km$	$8\ V/km$
BD	11	13	18	25	27	32

Table 5.10: Candidate transformers for BD placement for $E = 2\ V/km$ to $8\ V/km$ after optimization (genetic algorithm)

E (V/km)	Candidate Transformers for GIC Blocking Device Placement (Genetic Algorithm)
3	14 19 24 27 83 84 89 95 126 158 159
4	14 19 24 27 44 83 84 85 89 95 126 158 159
5	9 14 19 24 27 45 47 82 83 84 89 95 97 124 125 132 158 159
6	6 9 14 19 22 24 27 31 40 45 46 83 84 85 89 95 108 109 119 125 128 158 159
7	6 9 14 18 19 22 24 27 31 40 45 46 56 79 83 84 85 89 95 108 109 119 125 128 149 158 159
8	6 9 14 18 19 22 23 24 27 31 40 45 46 56 62 76 79 83 84 85 86 89 95 108 109 119 125 128 149 157 158 159

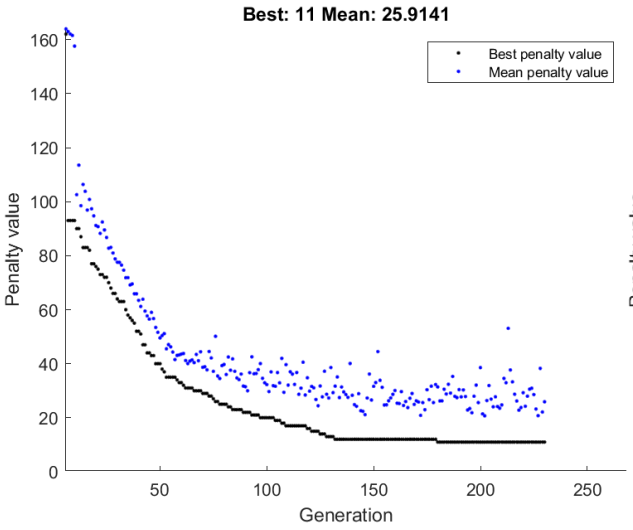

Figure 5.44: Best value at $E = 3\ V/km$ (genetic algorithm).

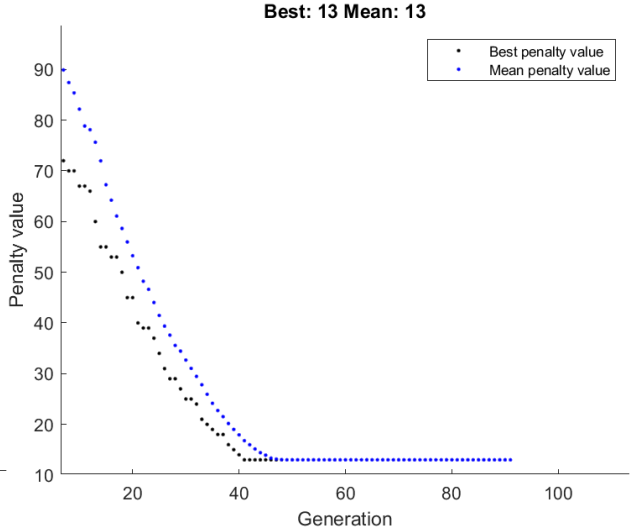

Figure 5.45: Best value at $E = 4\ V/km$ (genetic algorithm).

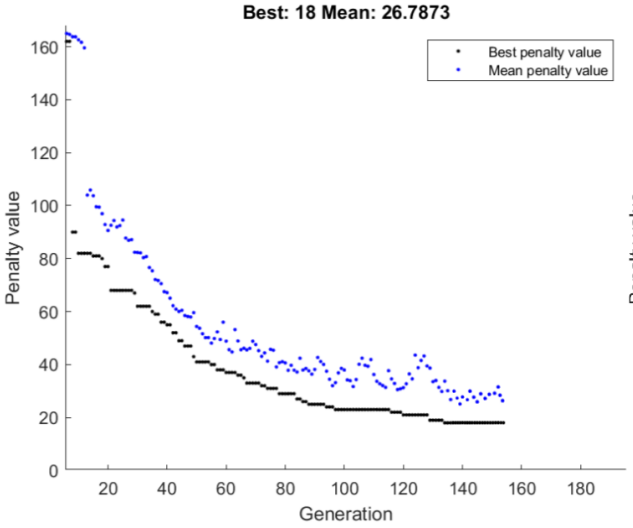

Figure 5.46: Best value at $E = 5\ V/km$ (genetic algorithm).

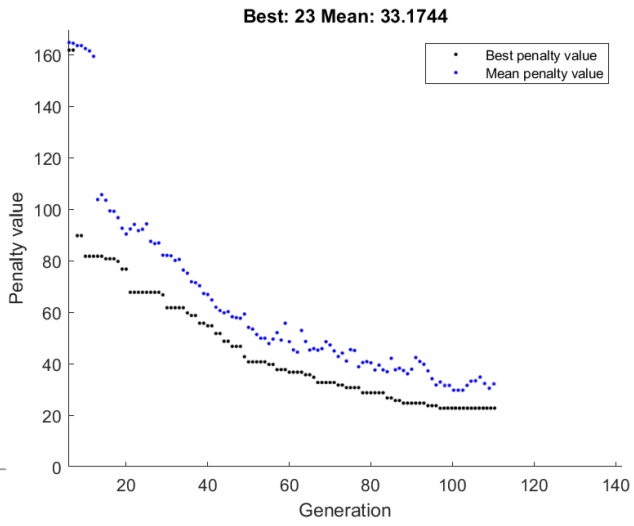

Figure 5.47: Best value at $E = 6\ V/km$ (genetic algorithm).

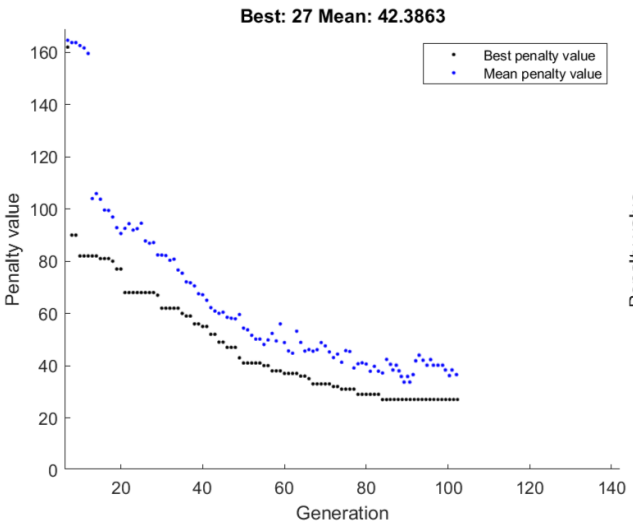

Figure 5.48: Best value at $E = 7\ V/km$ (genetic algorithm).

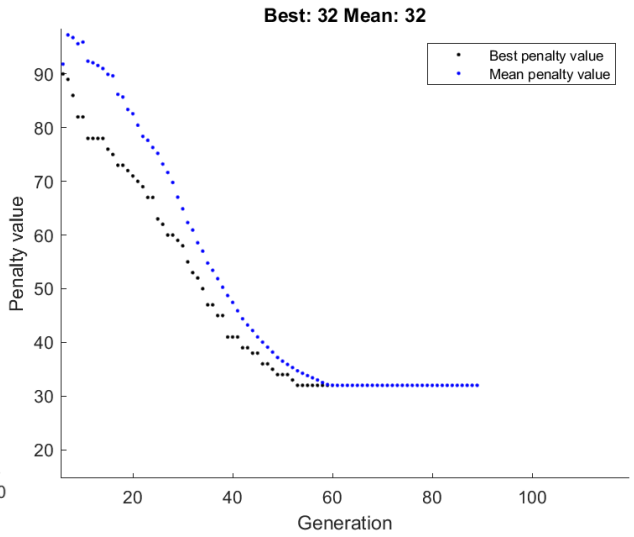

Figure 5.49: Best value at $E = 8\ V/km$ (genetic algorithm).

5.3.2.1 Results after BD placement (Genetic Algorithm)

Figure 5.50 to Figure 5.55 show the voltage at bus 115 and 53 after BD placement at different level of E ($E = 3\,V/km$ to $8\,V/km$) using genetic algorithm. At $E = 3\,V/km$, the minimum voltage of bus 115 is increased above $0.94 p.u.$ and is $0.9603 p.u.$ after placing BDs as mentioned in Table 5.10. However, bus 53 voltage reaches the minimum of $0.9397\,p.u.$, and to further increase it to above $0.94\,p.u.$; the load is decreased to 95% as it is more cost-effective than placing another BD. It is seen that the voltage is improved to $0.9404\,p.u.$ in Figure 5.50 and is in the acceptable range.

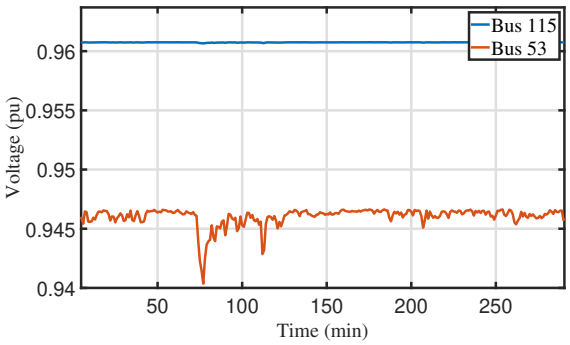

Figure 5.50: Voltage ($p.u.$) at bus 115 and 53 at $E = 3\,V/km$ (with BD, genetic algorithm).

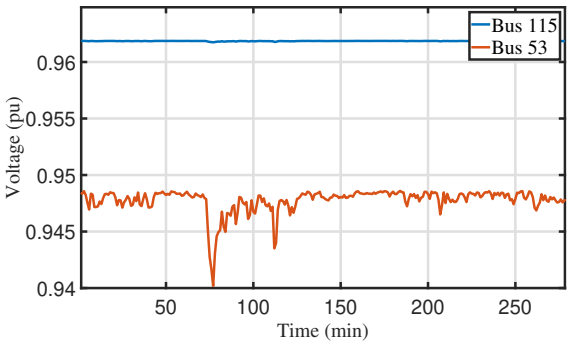

Figure 5.51: Voltage ($p.u.$) at bus 115 and 53 at $E = 4\,V/km$ (with BD, genetic algorithm).

At $E = 4V/km$, the minimum voltage at bus 115 is more than $0.94 p.u.$, but the minimum voltage at bus 53 was $0.9376\,p.u.$ after placing BDs mentioned in Table. 5.10. So, the total load is decreased to 80% to maintain the bus voltage of bus 53 above $0.94 p.u.$ and is improved to $0.9402\,p.u.$ as seen in Figure 5.51. Similarly, at $E = 5V/km$, after placing BDs, the minimum voltage at bus 115 is more than $0.94\,p.u.$, and the minimum voltage at bus 53 was

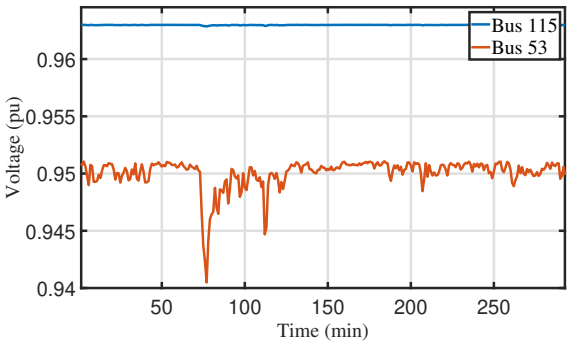

Figure 5.52: Voltage ($p.u.$) at bus 115 and 53 at $E = 5\,V/km$ (with BD, genetic algorithm).

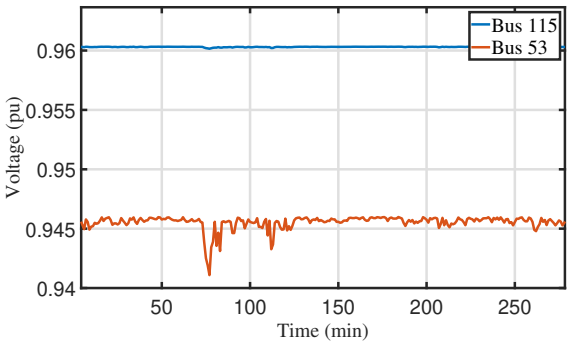

Figure 5.53: Voltage ($p.u.$) at bus 115 and 53 at $E = 6\,V/km$ (with BD, genetic algorithm).

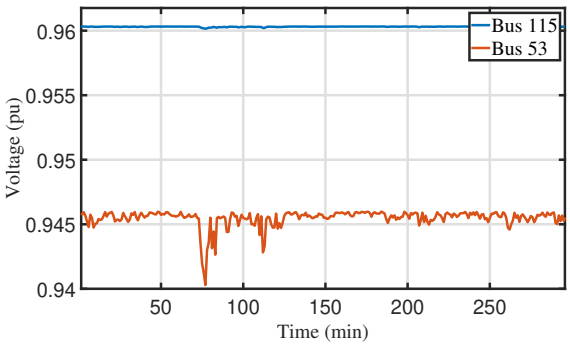

Figure 5.54: Voltage ($p.u.$) at bus 115 and 53 at $E = 7\,V/km$ (with BD, genetic algorithm).

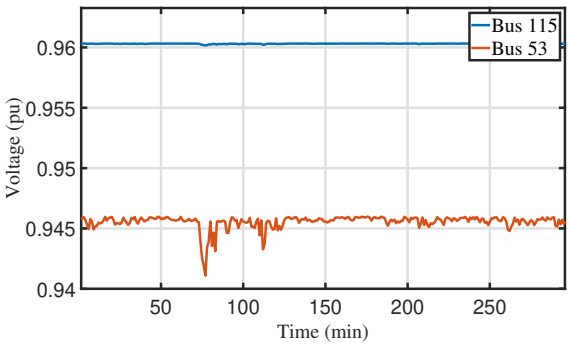

Figure 5.55: Voltage ($p.u.$) at bus 115 and 53 at $E = 8\,V/km$ (with BD, genetic algorithm).

0.9356 $p.u.$ So, the total load is decreased to 60% to maintain bus voltage at bus 53 above 0.94 $p.u.$ and is improved to 0.9405 $p.u.$ as seen in Figure 5.52. Placing BDs mentioned on Table 5.10 shows that the voltage improvement at $E = 6\,V/km$ after BD placement at the transformer neutrals is above 0.94 $p.u.$ for all buses as seen in Figure 5.53. Similarly, the voltage at all buses is more than minimum permissible voltage 0.94 $p.u.$ after placing BDs as

stated in the Table 5.10 for $E = 7\,V/km$ and $E = 8\,V/km$ which is also shown in Figure 5.54 and Figure 5.55.

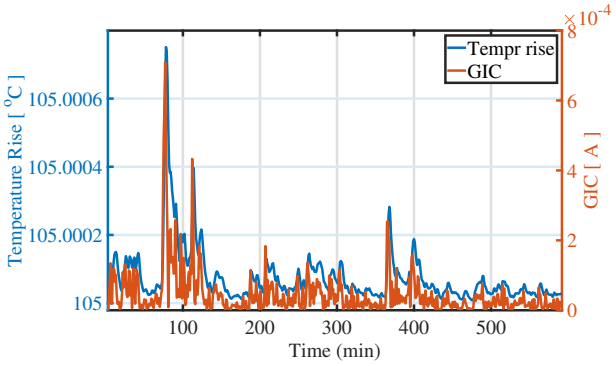

Figure 5.56: Temperature rise ($°C$) at transformer 19 tie-plate at $E = 3\,V/km$ (with BD, genetic algorithm).

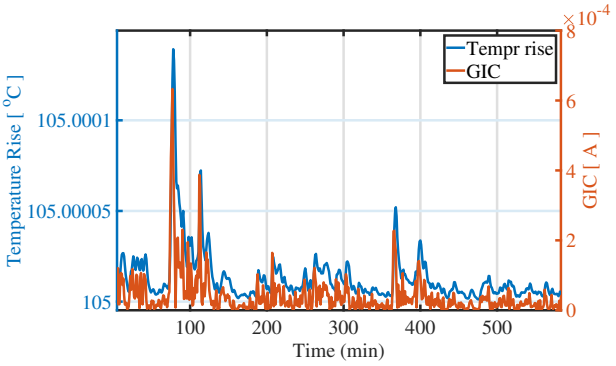

Figure 5.57: Temperature rise ($°C$) at transformer 19 winding at $E = 3\,V/km$ (with BD, genetic algorithm).

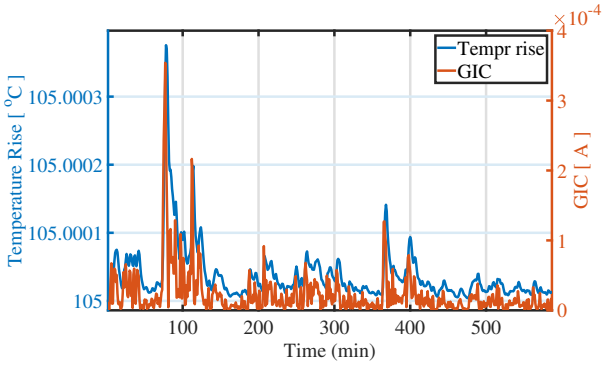

Figure 5.58: Temperature rise ($°C$) at transformer 19 tie-plate at $E = 6\,V/km$ (with BD, genetic algorithm).

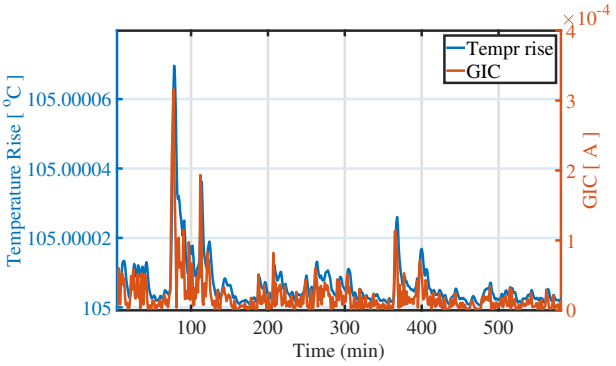

Figure 5.59: Temperature rise ($°C$) at transformer 19 winding at $E = 6\,V/km$ (with BD, genetic algorithm).

The hotspot temperature rise of the transformer number 19 after BD placement is decreased to much extent, and is shown in Figure 5.56 to Figure 5.61 for both tie-plate and winding of transformer at $E = 3\,V/km$, $6\,V/km$ and $8\,V/km$. The results of only $E = 3\,V/km$,

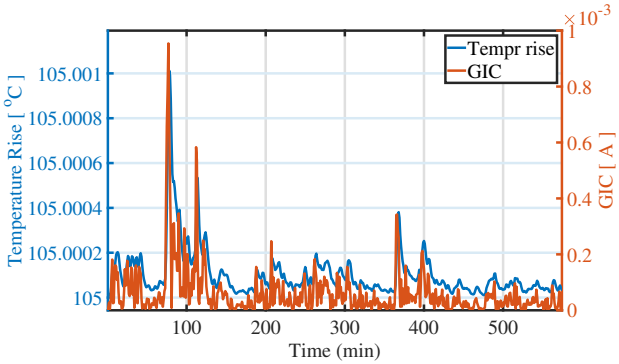

Figure 5.60: Temperature rise ($°C$) at transformer 19 tie-plate at $E = 8\,V/km$ (with BD, genetic algorithm).

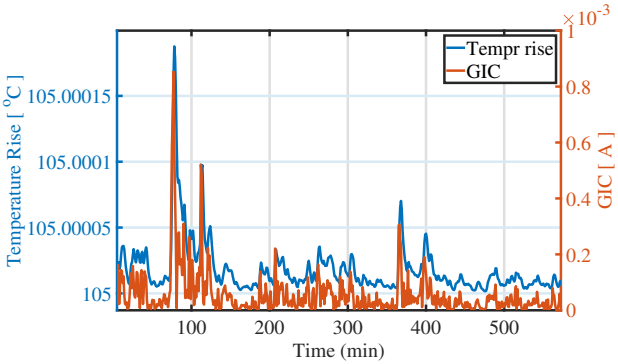

Figure 5.61: Temperature rise ($°C$) at transformer 19 winding at $E = 8\,V/km$ (with BD, genetic algorithm).

$6\,V/km$, and $8\,V/km$ are taken because the results for all E are similar as the GIC through the transformers is zero after placing BDs. Hence, the only temperature that is seen is the temperature of the top oil of the transformer, which is $105\,°C$.

5.4 Comparison of the results

As we can see from the tables and graphs resulting from surrogate optimization and genetic algorithm, the number of total GIC blocking devices to be placed at the neutral of transformers is higher in numbers in the genetic algorithm than in surrogate optimization. Also, the results from GA are presented such that they are the best-obtained results after several simulations. The main drawback of GA is that the program takes excessive time to run, i.e., two weeks on a regular workstation desktop, and every time the program is simulated, the results are different. However, with surrogate optimization, the time taken by the program was comparatively less, i.e., three days. The total number of BDs after optimization by surrogate optimization at

$E = 3\,V/km$ is 6, while the genetic algorithm is 11. The program was simulated four times for the genetic algorithm, and 11 was the lowest number that was obtained. While with surrogate optimization, every time the program is executed, 6 was the result. The candidate transformers resulting from surrogate optimization were also in the genetic algorithm, which has an additional five candidate transformers. For $E = 4\,V/km$, the number of BDs to be placed is the same with surrogate optimization and genetic algorithm, i.e., 13. However, the candidate transformers are somewhat different, with some common candidate transformers, it is elaborated in Table 5.12. Similarly, For $E = 5\,V/km$, the number of BDs in surrogate optimization is less than in the genetic algorithm, being 15 and 18, respectively, while some of the candidate transformers are similar. Furthermore, for $E = 6\,V/km$, the number of BDs in GA is higher than in SO, but the candidate transformers resulting from SO are all present in GA with additional candidate transformers. The same is for $E = 7\,V/km$ and $8\,V/km$; the total number of BDs resulting from GA is higher than SO, and candidates resulting from SO are all present in the results from GA. Overall, surrogate optimization is proved to be an effective solution for optimization as compared to genetic algorithm as the number of BDs is less with SO than GA for different levels of the geoelectric field; the computational time for GA for a given E is more than the computational time for SO and GA being stochastic in nature where the results obtained were different every time the program was executed for a same given E but this problem was not in the case of SO as same result was obtained for a given E.The total number of blocking devices obtained from both solvers is presented in Table 5.11, and a clear comparison between the two solvers is presented in Table 5.12.

Table 5.11: Total number of BDs for each solver

E (V/km)	Genetic Algorithm	Surrogate Optimization
3 (V/km)	11	6
4 (V/km)	13	13
5 (V/km)	18	15
6 (V/km)	25	19
7 (V/km)	27	24
8 (V/km)	32	28

Table 5.12: Comparison of Solvers and their Results

Genetic Algorithm (GA)	Surrogate Optimization (SO)
Total number of BDs from genetic algorithm is more than surrogate optimization.	Total number of BDs from surrogate optimization is less than genetic algorithm.
Different results for a given E each time the program is simulated.	Same result for a given E each time the program is simulated.
Does not converge to a global solution.	Converge to a global solution.
Takes excessive time to execute (two weeks) in normal workstation desktop.	Takes comparatively less time than GA (three days) in the same device.
GA takes more time because at each step, it selects individuals from the current population to be parents, and uses them to produce the children for the next generation. Over successive generations, the population "evolves" toward an optimal solution.	SO takes less time because it search for a point that minimizes an objective function, simply evaluate its surrogate on thousands of points, and take the best value as an approximation to the minimizer of the objective function.
Candidate transformers for E=3 V/km from GA is same as SO with additional candidates. Candidate transformers for E=4 V/km and E=5 V/km from GA are different than SO with the most vulnerable transformers among all being in both. However, other transformers vary because two solvers have different search procedure and work differently. Therefore, the optimal solution might be different but the constraints are satisfied from both solvers. Candidate transformers for E=6 V/km, 7V/km, and 8 V/km are same for both solvers with additional BDs in GA.	

Chapter 6

Conclusion and Future Work

6.1 Summary and Conclusion

The research in this thesis presents two methods of optimization to find the total number of blocking devices that are needed to be placed at the neutral of transformers to block the geomagnetically induced current caused by geomagnetical disturbance when large coronal mass ejections (CME) occur and are directed to the earth that perturbs earth's magnetic field and produces voltage at earth's surface which results in GIC. The thesis highlights the risks associated with the GIC being damage to the power system assets, typically transformers, and loss of reactive power support, causing voltage instability and power system collapse. The effects of GIC include half-cycle saturation that results in harmonic currents, magnetic flux flowing outside the core, and increased reactive power consumption. It can create heating in transformers, which, if sufficiently high and for a long duration, can cause damage to the

transformers and insulation breakdown.

As discussed in chapter 5, the most likely and negative effects of GMD are increased reactive power consumption and voltage instability, and overheating of power transformers. Restoration from power system collapse would be a matter of hours to days but replacing transformers requires months and excessive cost. Monitoring unusual voltage and reactive power swings, monitoring abnormal temperature rise, noise in transformers, and measuring GICs and harmonic currents are some of the mitigation approaches for GIC, while placing GIC blocking devices at the transformers neutral to ground connection is one potential mitigation approach to mitigate GIC. As a whole, the thesis provides the optimized number of blocking devices to be placed for blocking GIC.

In Chapter 2, the detailed literature review on geomagnetically induced current and its consequences in power systems are well explained. The insights on blocking devices are also provided, including why BDs are necessary and how this work can help solve the problem. The thesis addresses the gap that although enough research has been done on the impacts of GIC and the placement of blocking devices, there is not enough research on the optimal placement of BDs. With a couple of papers on the optimized placement of BDs, transformers' hotspot temperature rise is not considered in any of the papers while finding the solution.

In Chapter 3, power system analysis is done under GIC conditions. Using standard circuit analysis techniques, GIC flowing in each line and each transformer is calculated. After calculating GIC, the reactive power loss of the transformers as a result of GIC is calculated and is represented as the reactive load connected to the transformer bus, and power flow analysis is performed with the updated reactive power at the bus. After calculating GIC through the transformers, each transformer's tie-plate and winding hotspot temperature rise

due to GIC is calculated. This chapter presents the maximum temperature limits that should not be exceeded to avoid severe damage to the transformers, that is $180\,^{\circ}C$ for winding and $200\,^{\circ}C$ for tie-plate of transformers. The study system of the 118-bus standard test system, including the GPS coordinates of the substation locations, and coordinates of the ends of transmission lines, are presented in this chapter. Other data includes transformer data with their rated MVA and respective connected bus.

In Chapter 4, the problem for optimization of blocking device placement is formulated. This chapter explains the optimization problem with two constraints considered, which are voltage constraint and transformer hotspot temperature constraint. The bus voltage should be above the minimum permissible voltage $0.94\,p.u.$, and the hotspot temperature of transformer tie-plate and winding should be less than $200\,^{\circ}C$ and $180\,^{\circ}C$ respectively.

Chapter 5 provides the results from the program simulation, such as the voltage drop at different buses during the condition of geomagnetic disturbance, hotspot temperature rise of transformers tie-plate and windings, the optimization results from surrogate optimization and genetic algorithm from MATLAB optimization toolbox, the improvement in voltage profile after BD placement and maintenance of temperature at transformer hotspot. The results from optimization includes the total number of BDs and the candidate transformers to which the BDs are placed at their neutral.

The contributions of the thesis include:

- The transformers are differentiated into the ones that are assumed to be repaired or replaced based on the temperature rise of transformer tie-plate and windings. If the transformer's hotspot temperature rise is more than 1.5 times the maximum limit,

then the transformers are assumed to be replaced; otherwise, they are repaired if the temperature rise is more than the maximum limit. This provides a realistic criterion to calculate the total cost based on the cost of repair and replacement of transformers as presented in chapter 3.

- Penalties are added to the cost function for each constraint violation and are based on the transformer repair or replacement. The optimization solvers surrogate optimization and genetic algorithm are chosen after reviewing and researching multiple methods in the MATLAB optimization toolbox. The algorithm of both methods are also presented in chapter 4.

- The results include the total number of BDs to be placed and the candidate transformers for BD placement from two methods, surrogate optimization, and genetic algorithm. To limit the overall cost as low as possible, the total load is decreased to some extent for different levels of the geoelectric field E such that the bus voltages are maintained above the minimum permissible voltage, and an extra number of BDs are avoided. The total load is decreased to 95% at $E = 3V/km$, 80% at $E = 4V/km$, and 60% at $E = 5V/km$, whereas for higher E, an additional BD is required.

- It is concluded that the total number of BDs obtained from surrogate optimization is less than the total number of BDs obtained from genetic algorithm for all levels of geoelectric field (E) except $E = 4V/km$ as presented in Table 5.11. Genetic algorithm is stochastic in nature, with different results obtained with each program execution for given E and fails to converge to the global minimum at times. GA taking an excessive amount of time to execute than surrogate optimization is another disadvantage. Whereas surrogate optimization converges to a global solution, and the solution obtained with

each execution is the same for given E. It took comparatively less time to evaluate than GA as well. So, as a whole, surrogate optimization is proved to be an effective and efficient method for the optimization process.

6.2 Future Work

There is still room for research on the optimal placement of blocking devices as very little research has been done yet. Surrogate optimization and genetic algorithm take high computational time (three days for surrogate optimization and two weeks for genetic algorithm in a normal workstation desktop). This is a considerable disadvantage when the time is limited. Other optimization methods could be proposed that do not take excessive time. While formulating the optimization problem, generators' maximum active power limits and reactive power limits could be used as extra constraints for a more effective solution. A more realistic penalty value for voltage violation could be taken for optimization problem formulation.

Bibliography

[1] "Geomagnetic Disturbances: Their Impact on the Power Grid". In: *IEEE Power and Energy Magazine* 11.4 (2013), pp. 71–78. DOI: 10.1109/MPE.2013.2256651.

[2] "Effects of geomagnetic disturbances on the bulk power systems". In: *North American Electric Reliability Corporation (NERC), Special Reliability Assessment Interim Report* (2012).

[3] P.R. Price. "Geomagnetically induced current effects on transformers". In: *IEEE Transactions on Power Delivery* 17.4 (2002), pp. 1002–1008. DOI: 10.1109/TPWRD.2002.803710.

[4] Afshin Rezaei-Zare. "Reactive Power Loss Versus GIC Characteristic of Single-Phase Transformers". In: *IEEE Transactions on Power Delivery* 30.3 (2015), pp. 1639–1640. DOI: 10.1109/TPWRD.2015.2394311.

[5] L. Bolduc et al. "Development of a DC current-blocking device for transformer neutrals". In: *IEEE Transactions on Power Delivery* 20.1 (2005), pp. 163–168. DOI: 10.1109/TPWRD.2004.835437.

[6] Hao Zhu and Thomas J. Overbye. "Blocking Device Placement for Mitigating the Effects of Geomagnetically Induced Currents". In: *IEEE Transactions on Power Systems* 30.4 (2015), pp. 2081–2089. DOI: 10.1109/TPWRS.2014.2357213.

[7] J.G. Kappenman et al. "GIC mitigation: a neutral blocking/bypass device to prevent the flow of GIC in power systems". In: *IEEE Transactions on Power Delivery* 6.3 (1991), pp. 1271–1281. DOI: 10.1109/61.85876.

[8] J G Kappenman. "Mitigation of geomagnetically induced and dc stray currents. Final report". In: (). URL: https://www.osti.gov/biblio/5259365.

[9] Amir H. Etemadi and Afshin Rezaei-Zare. "Optimal Placement of GIC Blocking Devices for Geomagnetic Disturbance Mitigation". In: *IEEE Transactions on Power Systems* 29.6 (2014), pp. 2753–2762. DOI: 10.1109/TPWRS.2014.2309004.

[10] Xiaoliang Ning et al. "Research on Optimal placement for GIC mitigation with Blocking Device". In: vol. 533. Institute of Physics Publishing, 2019. DOI: 10.1088/1757-899X/533/1/012042.

[11] *Geo-magnetic Disturbances (GMD): Monitoring, Mitigation, and Next Steps*. 2011. URL: www.epri.com.

[12] R. Girgis and Kiran Vedante. "Effects of GIC on power transformers and power systems". In: May 2012, pp. 1–8. ISBN: 978-1-4673-1934-8. DOI: 10.1109/TDC.2012.6281595.

[13] David Boteler. "Geomagnetic Hazards to Conducting Networks". In: *Natural Hazards* 28 (Mar. 2003), pp. 537–561. DOI: 10.1023/A:1022902713136.

[14] J.N. Wrubel. "Monitoring for geomagnetic induced current flow effects using existing EMS telemetering". In: *[Proceedings] Conference Papers 1991 Power Industry Computer Application Conference*. 1991, pp. 45–49. DOI: 10.1109/PICA.1991.160652.

[15] David H. Boteler. "The Evolution of Québec Earth Models Used to Model Geomagnetically Induced Currents". In: *IEEE Transactions on Power Delivery* 30.5 (2015), pp. 2171–2178. DOI: 10.1109/TPWRD.2014.2379260.

[16] Leonard Bolduc. "GIC observations and studies in the Hydro-Quebec power system". In: *Journal of Atmospheric and Solar-Terrestrial Physics* 64 (2002), pp. 1793–1802. URL: www.elsevier.com/locate/jastp.

[17] R. Tozzi et al. "A Preliminary Risk Assessment of Geomagnetically Induced Currents over the Italian Territory". In: *Space Weather* 17 (1 Jan. 2019), pp. 46–58. ISSN: 15427390. DOI: 10.1029/2018SW002065.

[18] R. A. Marshall et al. "A preliminary risk assessment of the Australian region power network to space weather". In: *Space Weather* 9 (10 2011). ISSN: 15427390. DOI: 10.1029/2011SW000685.

[19] Turhan Demiray, Giovanni Beccuti, and Göran Andersson. "Risk assessment of the impact of geomagnetic disturbances on the transmission grid in Switzerland". In: 2013. ISBN: 9781479913039. DOI: 10.1109/PESMG.2013.6672600.

[20] "The global risk continuum (GRC)". In: *Journal of Space Safety Engineering* 7 (1 Mar. 2020), pp. 38–43. ISSN: 24688967. DOI: 10.1016/j.jsse.2020.01.002.

[21] W. A. Radasky and J. G. Kappenman. "Impacts of geomagnetic storms on EHV and UHV power grids". In: *2010 Asia-Pacific International Symposium on Electromagnetic Compatibility*. 2010, pp. 695–698. DOI: 10.1109/APEMC.2010.5475523.

[22] L. Trichtchenko and D.H. Boteler. "Effects of Recent Geomagnetic Storms on Power Systems". In: *2007 7th International Symposium on Electromagnetic Compatibility and Electromagnetic Ecology*. 2007, pp. 265–268. DOI: 10.1109/EMCECO.2007.4371706.

[23] Kuan Zheng et al. "Effects of Geophysical Parameters on GIC Illustrated by Benchmark Network Modeling". In: *IEEE Transactions on Power Delivery* 28.2 (2013), pp. 1183–1191. DOI: 10.1109/TPWRD.2013.2249119.

[24] Pooria Dehghanian et al. "System-Wide Case Study Assessment of Transformer Heating Due to Geomagnetic Disturbances". In: *2019 North American Power Symposium (NAPS)*. 2019, pp. 1–6. DOI: 10.1109/NAPS46351.2019.8999983.

[25] Komal Shetye and Tom Overbye. "Modeling and Analysis of GMD Effects on Power Systems: An overview of the impact on large-scale power systems." In: *IEEE Electrification Magazine* 3.4 (2015), pp. 13–21. DOI: 10.1109/MELE.2015.2480356.

[26] Afshin Rezaei-Zare. "Behavior of Single-Phase Transformers Under Geomagnetically Induced Current Conditions". In: *IEEE Transactions on Power Delivery* 29.2 (2014), pp. 916–925. DOI: 10.1109/TPWRD.2013.2281516.

[27] R.A. Walling and A.N. Khan. "Characteristics of transformer exciting-current during geomagnetic disturbances". In: *IEEE Transactions on Power Delivery* 6.4 (1991), pp. 1707–1714. DOI: 10.1109/61.97710.

[28] Hanli Weng et al. "The impact of GIC on system voltage and generator output". In: *2015 5th International Conference on Electric Utility Deregulation and Restructuring and Power Technologies (DRPT)*. 2015, pp. 1736–1739. DOI: 10.1109/DRPT.2015.7432514.

[29] Sakis Meliopoulos, Jiahao Xie, and George Cokkinides. "Power system harmonic analysis under geomagnetic disturbances". In: *2018 18th International Conference on Harmonics and Quality of Power (ICHQP)*. 2018, pp. 1–6. DOI: 10.1109/ICHQP.2018.8378913.

[30] Luis Marti, Afshin Rezaei-Zare, and Arun Narang. "Simulation of Transformer Hotspot Heating due to Geomagnetically Induced Currents". In: *IEEE Transactions on Power Delivery* 28.1 (2013), pp. 320–327. DOI: 10.1109/TPWRD.2012.2224674.

[31] S. Arabi, M. M. Komaragiri, and M. Z. Tarnawecky. "Effects of geomagnetically-induced currents in power transformers from power systems point of view". In: *Canadian Electrical Engineering Journal* 12.4 (1987), pp. 165–170. DOI: 10.1109/CEEJ.1987.6591093.

[32] C. T Gaunt and G. Coetzee. "Transformer failures in regions incorrectly considered to have low GIC-risk". In: *2007 IEEE Lausanne Power Tech*. 2007, pp. 807–812. DOI: 10.1109/PCT.2007.4538419.

[33] R.S. Girgis and C.-D. Ko. "Calculation techniques and results of effects of GIC currents as applied to large power transformers". In: *IEEE Transactions on Power Delivery* 7.2 (1992), pp. 699–705. DOI: 10.1109/61.127070.

[34] John Kappenman. *Low-Frequency Protection Concepts for the Electric Power Grid: Geomagnetically Induced Current (GIC) and E3 HEMP Mitigation*. 2010.

[35] Moazzam Nazir, Johan H. Enslin, and Mohammad Babakmehr. "Power System Protection response under Geomagnetically Induced Currents". In: *2020 Clemson University Power Systems Conference (PSC)*. 2020, pp. 1–6. DOI: 10.1109/PSC50246.2020.9131172.

[36] "IEEE Guide for Loading Mineral-Oil-Immersed Transformers and Step-Voltage Regulators". In: *IEEE Std C57.91-2011 (Revision of IEEE Std C57.91-1995)* (2012), pp. 1–123. DOI: 10.1109/IEEESTD.2012.6166928.

[37] D.H. Boteler et al. "Real-Time Simulation of Geomagnetically Induced Currents". In: *2007 7th International Symposium on Electromagnetic Compatibility and Electromagnetic Ecology*. 2007, pp. 261–264. DOI: 10.1109/EMCECO.2007.4371705.

[38] Mark D Butala et al. "Modeling geomagnetically induced currents from magnetometer measurements: Spatial scale assessed with reference measurements". In: *Space Weather* 15.10 (2017), pp. 1357–1372.

[39] Aboutaleb Haddadi et al. "A Modified IEEE 118-Bus Test Case for Geomagnetic Disturbance Studies–Part I: Model Data". In: *IEEE Transactions on Electromagnetic Compatibility* 62.3 (2020), pp. 955–965. DOI: 10.1109/TEMC.2019.2920271.

[40] G. Swift, T.S. Molinski, and W. Lehn. "A fundamental approach to transformer thermal modeling. I. Theory and equivalent circuit". In: *IEEE Transactions on Power Delivery* 16.2 (2001), pp. 171–175. DOI: 10.1109/61.915478.

[41] *Magnetohydrodynamic Electromagnetic Pulse Assessment of the Continental U.S. Electric Grid Geomagnetically Induced Current and Transformer Thermal Analysis*. URL: www.epri.com.

[42] Thomas J. Overbye et al. "Integration of geomagnetic disturbance modeling into the power flow: A methodology for large-scale system studies". In: *2012 North American Power Symposium (NAPS)*. 2012, pp. 1–7. DOI: 10.1109/NAPS.2012.6336365.

[43] *Monitoring and Mitigation of Geomagnetically Induced Currents*. 2008. URL: www.epri.com.

[44] John Kappenman. *Geomagnetic Storms and Their Impacts on the U.S. Power Grid*. 2010.

[45] Richard Lordan. *Geomagnetic Disturbance (GMD) Neutral Blocking Device Analysis*. 2014. URL: www.epri.com.

[46] PB Kotzé, PJ Cilliers, and PR Sutcliffe. "The role of SANSA's geomagnetic observation network in space weather monitoring: A review". In: *Space Weather* 13.10 (2015), pp. 656–664.

[47] Marcelo Zapella et al. "Solving old problems with new technology: How to monitor and measure GIC and OPD currents". In: *2018 71st Annual Conference for Protective Relay Engineers (CPRE)*. 2018, pp. 1–8. DOI: 10.1109/CPRE.2018.8349825.

[48] Chumki Basu et al. "Combining multiple sources of data for situational awareness of geomagnetic disturbances". In: *2015 IEEE Power Energy Society General Meeting*. 2015, pp. 1–5. DOI: 10.1109/PESGM.2015.7286179.

[49] Maryam Kazerooni et al. "Estimation of geoelectric field for validating geomagnetic disturbance modeling". In: *2013 IEEE Power and Energy Conference at Illinois (PECI)*. 2013, pp. 218–224. DOI: 10.1109/PECI.2013.6506061.

[50] Cecilia Klauber and Hao Zhu. "Power network topology control for mitigating the effects of geomagnetically induced currents". In: *2016 50th Asilomar Conference on Signals, Systems and Computers*. 2016, pp. 313–317. DOI: 10.1109/ACSSC.2016.7869049.

[51] Afshin Rezaei-Zare and Amir H. Etemadi. "Optimal Placement of GIC Blocking Devices Considering Equipment Thermal Limits and Power System Operation Constraints". In: *IEEE Transactions on Power Delivery* 33.1 (2018), pp. 200–208. DOI: 10.1109/TPWRD.2017.2711502.

[52] I. A. Erinmez, John G. Kappenman, and William A. Radasky. "Management of the geomagnetically induced current risks on the national grid company's electric power transmission system". In: *Journal of Atmospheric and Solar-Terrestrial Physics* 64 (2002), pp. 743–756.

[53] Moazzam Nazir, Klaehn Burkes, and Johan H. Enslin. "Electrical Safety Considerations of Neutral Blocker Placements for Mitigating DC". In: *IEEE Transactions on Industry Applications* 57.1 (2021), pp. 1113–1121. DOI: 10.1109/TIA.2020.3032081.

[54] Mowen Lu et al. "Optimal Transmission Line Switching Under Geomagnetic Disturbances". In: *IEEE Transactions on Power Systems* 33.3 (2018), pp. 2539–2550. DOI: 10.1109/TPWRS.2017.2761178.

[55] Esko Arajärvi, Risto Pirjola, and Ari Viljanen. "Effects of neutral point reactors and series capacitors on geomagnetically induced currents in a high-voltage electric power transmission system". In: *Space Weather* 9.11 (2011). DOI: https://doi.org/10.1029/2011SW000715. URL: https://agupubs.onlinelibrary.wiley.com/doi/abs/10.1029/2011SW000715.

[56] D.H. Boteler. "Calculating the voltages induced in technological systems during a geomagnetic disturbance". In: *IEEE Transactions on Electromagnetic Compatibility* 41.4 (1999), pp. 398–402. DOI: 10.1109/15.809834.

[57] Randy Horton et al. "A Test Case for the Calculation of Geomagnetically Induced Currents". In: *IEEE Transactions on Power Delivery* 27.4 (2012), pp. 2368–2373. DOI: 10.1109/TPWRD.2012.2206407.

[58] Richard H Rapp. *Geometric Geodesy Part I*. Ohio State University Department of Geodetic Science and Surveying, 1991.

[59] V. D. Albertson et al. "Load-Flow Studies in the Presence of Geomagnetically-Induced Currents". In: *IEEE Transactions on Power Apparatus and Systems* PAS-100.2 (1981), pp. 594–607. DOI: 10.1109/TPAS.1981.316916.

[60] D.H. Boteler and R.J. Pirjola. "Modelling geomagnetically induced currents produced by realistic and uniform electric fields". In: *IEEE Transactions on Power Delivery* 13.4 (1998), pp. 1303–1308. DOI: 10.1109/61.714500.

[61] Xuzhu Dong, Yilu Liu, and J.G. Kappenman. "Comparative analysis of exciting current harmonics and reactive power consumption from GIC saturated transformers". In: *2001 IEEE Power Engineering Society Winter Meeting. Conference Proceedings (Cat. No.01CH37194)*. Vol. 1. 2001, 318–322 vol.1. DOI: 10.1109/PESW.2001.917055.

[62] Afshin Rezaei-Zare. "Enhanced Transformer Model for Low- and Mid-Frequency Transients—Part I: Model Development". In: *IEEE Transactions on Power Delivery* 30.1 (2015), pp. 307–315. DOI: 10.1109/TPWRD.2014.2347930.

[63] Afshin Rezaei-Zare. "Enhanced Transformer Model for Low- and Mid-Frequency Transients—Part II: Validation and Simulation Results". In: *IEEE Transactions on Power Delivery* 30.1 (2015), pp. 316–325. DOI: 10.1109/TPWRD.2014.2347934.

[64] Afshin Rezaei-Zare et al. "Analysis of Three-Phase Transformer Response due to GIC Using an Advanced Duality-Based Model". In: *IEEE Transactions on Power Delivery* 31.5 (2016), pp. 2342–2350. DOI: 10.1109/TPWRD.2015.2505499.

[65] *Assessment Guide: Geomagnetic Disturbance Harmonic Impacts and Asset Withstand Capabilities*. URL: www.epri.com.

[66] Shamsodin Taheri et al. "Effect of power system harmonics on transformer loading capability and hot spot temperature". In: 2012. ISBN: 9781467314336. DOI: 10.1109/CCECE.2012.6334834.

[67] Joe Perez. "Fundamental principles of transformer thermal loading and protection". In: *2010 63rd Annual Conference for Protective Relay Engineers*. 2010, pp. 1–14. DOI: 10.1109/CPRE.2010.5469518.

[68] DH Shroff and AW Stannett. "A review of paper aging in power transformers". In: *IEE Proceedings C (Generation, Transmission and Distribution)*. Vol. 132. 6. IET. 1985, pp. 312–319.

[69] H. Yoshida et al. "Degradation of Insulating Materials of Transformers". In: *IEEE Transactions on Electrical Insulation* EI-22.6 (1987), pp. 795–800. DOI: 10.1109/TEI.1987.298942.

[70] W.J. McNutt. "Insulation thermal life considerations for transformer loading guides". In: *IEEE Transactions on Power Delivery* 7.1 (1992), pp. 392–401. DOI: 10.1109/61.108933.

[71] Jawad Faiz and Milad Soleimani. "Dissolved gas analysis evaluation in electric power transformers using conventional methods a review". In: *IEEE Transactions on Dielectrics and Electrical Insulation* 24.2 (2017), pp. 1239–1248. DOI: 10.1109/TDEI.2017.005959.

[72] G. Swift et al. "A fundamental approach to transformer thermal modeling. II. Field verification". In: *IEEE Transactions on Power Delivery* 16.2 (2001), pp. 176–180. DOI: 10.1109/61.915479.

[73] Ramsis S. Girgis and Kiran B. Vedante. "Impact of GICs on Power Transformers: Overheating is not the real issue." In: *IEEE Electrification Magazine* 3.4 (2015), pp. 8–12. DOI: 10.1109/MELE.2015.2480355.

[74] R. Bouhaddiche, S. Bouazabia, and I. Fofana. "Thermal modelling of power transformer". In: *2017 IEEE 19th International Conference on Dielectric Liquids (ICDL)*. 2017, pp. 1–4. DOI: 10.1109/ICDL.2017.8124676.

[75] *Screening Criterion for Transformer Thermal Impact Assessment White Paper TPL-007-2 Transmission System Planned Performance for Geomagnetic Disturbance Events*.

[76] A. Pulkkinen et al. "Generation of 100-year geomagnetically induced current scenarios". In: *Space Weather* 10.4 (2012). DOI: https://doi.org/10.1029/2011SW000750. URL: https://agupubs.onlinelibrary.wiley.com/doi/abs/10.1029/2011SW000750.

[77] Edward J. Oughton et al. "A Risk Assessment Framework for the Socioeconomic Impacts of Electricity Transmission Infrastructure Failure Due to Space Weather: An Application to the United Kingdom". In: *Risk Analysis* 39.5 (), pp. 1022–1043. DOI: https://doi.org/10.1111/risa.13229.

[78] Afshin Rezaei-Zare et al. "Geomagnetic Disturbance (GMD) Transformer Thermal Analysis Tool: EPRI Transformer Thermal Model (ETTM), version 1.0-Beta Grid-tied Inverters View project Power System Test Cases for EMT-type Simulation Studies View project". In: (2018). DOI: 10.13140/RG.2.2.26826.62400. URL: https://www.researchgate.net/publication/331245789.

[79] G.W. Swift et al. "Adaptive transformer thermal overload protection". In: *IEEE Transactions on Power Delivery* 16.4 (2001), pp. 516–521. DOI: 10.1109/61.956730.

[80] *Transmission Cost Estimation Guide MTEP20*. 2020.

[81] Rich Christie. "Power systems test case archive". In: *University of Washington* (2013).

[82] *Global Optimization Toolbox User's Guide R2021b*. 2004. URL: www.mathworks.com.

[83] H.-M. Gutmann. "A Radial Basis Function Method for Global Optimization". In: *JOURNAL OF GLOBAL OPTIMIZATION* 19 (1999), p. 2001.

[84] Zhong-Hua Han and ke-shi Zhang. "Surrogate-Based Optimization". In: Mar. 2012. ISBN: 978-953-51-0146-8. DOI: 10.5772/36125.

[85] Melanie Mitchell. *An introduction to genetic algorithms*. MIT press, 1998.

[86] Gustavo Alonso, Edmundo del Valle, and Jose Ramon Ramirez. "Optimization methods". In: *Desalination in Nuclear Power Plants* (Jan. 2020), pp. 67–76. DOI: 10.1016/B978-0-12-820021-6.00005-3. URL: https://linkinghub.elsevier.com/retrieve/pii/B9780128200216000053.

Publication

CONFERENCE PAPER

Anusha Lamichhane, Afshin Rezaei-Zare and Ali Asgary, "Optimal Placement of GIC Blocking Devices Considering Transformer Thermal Limit Using Surrogate Optimization", 022 IEEE International Conference on Environment and Electrical Engineering and 2022 IEEE Industrial and Commercial Power Systems Europe (EEEIC / ICPS Europe), 2022.